TECHNICAL REPORT HL-88-27

SAN FRANCISCO BAY: MODELING SYSTEM FOR DREDGED MATERIAL DISPOSAL AND HYDRAULIC TRANSPORT

by

Virginia R. Pankow

Hydraulics Laboratory

DEPARTMENT OF THE ARMY
Waterways Experiment Station, Corps of Engineers
PO Box 631, Vicksburg, Mississippi 39181-0631

November 1988
Final Report

Prepared for US Army Engineer District, San Francisco
San Francisco, California 94105-1905

Unclassified
SECURITY CLASSIFICATION OF THIS PAGE

REPORT DOCUMENTATION PAGE

Form Approved OMB No. 0704-0188

1a. REPORT SECURITY CLASSIFICATION Unclassified	1b. RESTRICTIVE MARKINGS
2a. SECURITY CLASSIFICATION AUTHORITY	3. DISTRIBUTION/AVAILABILITY OF REPORT Approved for public release; distribution unlimited.
2b. DECLASSIFICATION/DOWNGRADING SCHEDULE	
4. PERFORMING ORGANIZATION REPORT NUMBER(S) Technical Report HL-88-27	5. MONITORING ORGANIZATION REPORT NUMBER(S)
6a. NAME OF PERFORMING ORGANIZATION USAEWES Hydraulics Laboratory 6b. OFFICE SYMBOL (*If applicable*) CEWES-HE-E	7a. NAME OF MONITORING ORGANIZATION
6c. ADDRESS (*City, State, and ZIP Code*) PO Box 631 Vicksburg, MS 39181-0631	7b. ADDRESS (*City, State, and ZIP Code*)
8a. NAME OF FUNDING/SPONSORING ORGANIZATION USAED, San Francisco 8b. OFFICE SYMBOL (*If applicable*)	9. PROCUREMENT INSTRUMENT IDENTIFICATION NUMBER
8c. ADDRESS (*City, State, and ZIP Code*) 211 Main Street San Francisco, CA 94105-1905	10. SOURCE OF FUNDING NUMBERS PROGRAM ELEMENT NO. / PROJECT NO. / TASK NO. / WORK UNIT ACCESSION NO.

11. TITLE (*Include Security Classification*)
San Francisco Bay: Modeling System for Dredged Material Disposal and Hydraulic Transport

12. PERSONAL AUTHOR(S)
Pankow, Virginia R.

13a. TYPE OF REPORT	13b. TIME COVERED	14. DATE OF REPORT (*Year, Month, Day*)	15. PAGE COUNT
Final report	FROM _____ TO _____	November 1988	84

16. SUPPLEMENTARY NOTATION
Available from National Technical Information Service, 5285 Port Royal Road, Springfield, VA 22161.

17. COSATI CODES			18. SUBJECT TERMS (*Continue on reverse if necessary and identify by block number*)
FIELD	GROUP	SUB-GROUP	Dredged material disposal models Dredged material management Hydrodynamic models (Continued)

19. ABSTRACT (*Continue on reverse if necessary and identify by block number*)

A combination of physical and numerical models was used to simulate the hydrodynamic, circulation, and sediment transport characteristics of San Francisco and San Pablo bays. This simulation was done in response to a request by the US Army Engineer District, San Francisco, to develop a modeling tool that can define the fate of dredged material disposed at the Alcatraz disposal site.

Tide and current velocity data from the San Francisco Bay-Delta physical model were used to verify the vertically averaged hydrodynamic model, RMA-2V (Two-Dimensional Model for Free Surface Flows). This model was used to generate the velocity field for a dredged material disposal model, DIFID (Discharge From an Instantaneous Dump). The suspended sediment concentrations from DIFID and the geometry and hydrodynamic data from RMA-2V were used in the sediment transport model, STUDH (Sediment Transport in Unsteady (Continued)

20. DISTRIBUTION/AVAILABILITY OF ABSTRACT	21. ABSTRACT SECURITY CLASSIFICATION
☒ UNCLASSIFIED/UNLIMITED ☐ SAME AS RPT ☐ DTIC USERS	Unclassified
22a. NAME OF RESPONSIBLE INDIVIDUAL	22b. TELEPHONE (*Include Area Code*) / 22c. OFFICE SYMBOL

DD Form 1473, JUN 86 *Previous editions are obsolete* SECURITY CLASSIFICATION OF THIS PAGE
Unclassified

18. SUBJECT TERMS (Continued).

Mathematical models
Physical models
San Francisco Bay
Sediment transport models

19. ABSTRACT (Continued).

Two-Dimensional Flows, Horizontal Plane), to establish sediment transport and dispersion patterns around the Alcatraz disposal site in central San Francisco Bay. Two model meshes were developed for this study: a comprehensive or global mesh of the entire system, and a more detailed inset mesh of the Alcatraz disposal area.

The modeling system has its capabilities and applications. However, the results are just reasonable simulations, not fully verified ones. Each of the numerical models, RMA-2V, DIFID, and STUDH, has individual capabilities and limitations, the greatest of which is the two-dimensional approximation of a three-dimensional phenomenon. The vertically averaged velocities and sediment fields will mask two-layer flow and other three-dimensional processes. Even with this simplification, the model results are useful in estimating the short- and long-term fates of sediments released during a disposal operation.

Appendix A describes the TABS-2 modeling system in which RMA-2V and STUDH belong, and Appendix B gives details of the numerical model DIFID.

PREFACE

The Alcatraz disposal modeling work described in this report was performed for the US Army Engineer District, San Francisco (SPN), Planning/ Engineering Division, as part of the District's Dredged Material Disposal Management Program.

The numerical simulations portion of the study was conducted in the Hydraulics Laboratory (HL) of the US Army Engineer Waterways Experiment Station (WES) during the period October 1986 to March 1988 under the general supervision of Messrs. Frank A. Herrmann, Chief, HL; Richard A. Sager, Assistant Chief, HL; William H. McAnally, Jr., Chief, Estuaries Division; and William D. Martin, Chief, Estuarine Engineering Branch.

The HL work was performed by Mmes. Paula G. Kee and Virginia R. Pankow, Estuarine Engineering Branch, under the technical guidance of Messrs. Michael J. Trawle, Waterways Division, and Allen M. Teeter, Estuarine Processes Branch, Estuaries Division, former and present Project Managers. Dr. Billy H. Johnson, Math Modeling Group, Waterways Division, and Ms. Barbara P. Donnell, Estuarine Simulation Branch, Estuaries Division, provided advice and assistance with the DIFID and TABS-2 models. Additional modeling support was provided by Mr. Julian M. Savage, Estuarine Processes Branch. Appendix A was written by the HL staff, and Appendix B was written by Mr. Trawle and Dr. Johnson. This report was prepared by Ms. Pankow and edited by Mrs. Marsha C. Gay, Information Technology Laboratory, WFS.

Mr. Brian Walls was SPN liaison during the study, and Mr. Thomas Wakeman, Model Director, SPN, supervised the work performed at the San Francisco Bay-Delta Model. Mr. Lester Tong, SPN, is Program Manager of the Dredged Material Disposal Management Program.

COL Dwayne G. Lee, EN, is the Commander and Director of WES. Dr. Robert W. Whalin is the Technical Director.

CONTENTS

CONVERSION FACTORS, NON-SI TO SI (METRIC)
UNITS OF MEASUREMENT

Non-SI units of measurement used in this report can be converted to SI (metric) units as follows:

Multiply	By	To Obtain
acres	4,046.873	square metres
cubic feet	0.02831685	cubic metres
cubic yards	0.7645549	cubic metres
feet	0.3048	metres
miles (US nautical)	1.852	kilometres
miles (US statute)	1.609347	kilometres
pounds (force)-second per square foot	47.88026	pascals-second
square feet	0.09290304	square metres

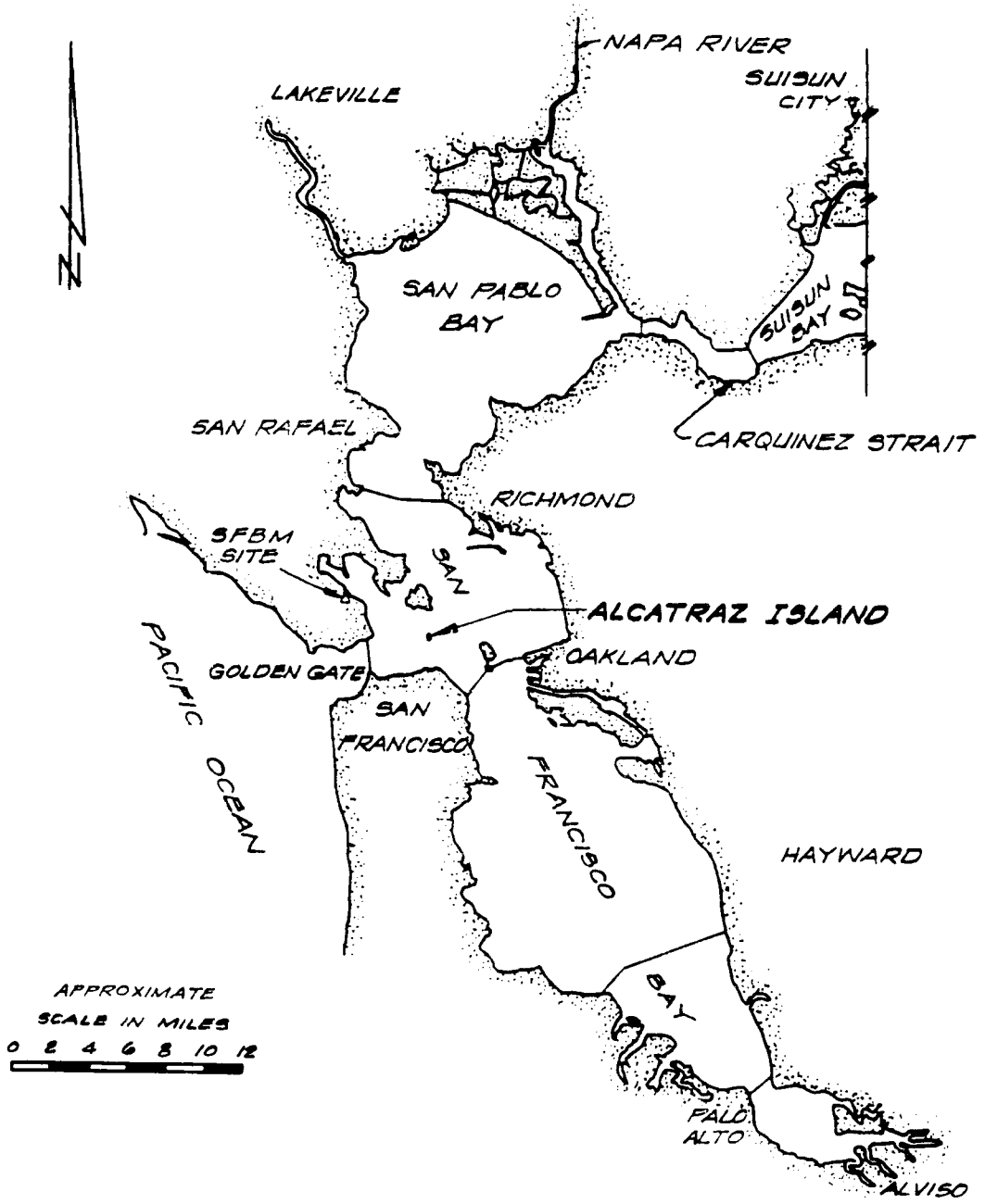

Figure 1. Location map

SAN FRANCISCO BAY: MODELING SYSTEM FOR DREDGED MATERIAL DISPOSAL AND HYDRAULIC TRANSPORT

PART I: INTRODUCTION

Background

1. The Alcatraz disposal site near Alcatraz Island is a naturally deep open-water site in San Francisco Bay (Figure 1). This has been used as a dispersive site for dredged material since the turn of the century. As such, material disposed there is intended to be transported out of the site toward the Golden Gate Bridge and out to sea by the strong tidal currents.

2. In 1982 personnel of the US Army Engineer District (USAED), San Francisco, discovered that the dredged materials being disposed at the Alcatraz site were not being dispersed at the rate that they were being introduced and that a permanent mound was forming. This mound was a hazard to navigation and indicated that the capacity of the disposal site was being taxed. There was also concern that more expensive alternate disposal sites would have to be developed in the future.

3. In response to the problem, USAED, San Francisco, formed the Dredged Material Disposal Management Program (DMP), which was tasked to (a) determine the fate of disposed material at the Alcatraz disposal site, and (b) develop modeling tools to assess disposal of dredged materials at various other locations in San Francisco Bay. A request was made to the US Army Engineer Waterways Experiment Station for assistance with these goals.

Objective

4. The overall objective of the disposal modeling study is to assist USAED, San Francisco, to meet the goals of the DMP by the development of a modeling tool that can define the fate of dredged material disposed at the Alcatraz disposal site. The purpose of this report is to describe and summarize the activities involved in the development and validation of the models used in this study and to demonstrate the capability of STUDH (Sediment

Transport in Unsteady Two-Dimensional Flows, Horizontal Plane), the sediment transport model.

Approach

5. The study objective was met through the use of both physical and numerical modeling techniques. This San Francisco Bay hybrid modeling approach consisted of the following interrelated parts:

a. The creation of a large-scale or comprehensive numerical model of the San Francisco Bay to simulate the hydrodynamic characteristics of the entire bay system. This numerical model was used to define tidal hydrodynamics and overall circulation patterns.

b. The use of the San Francisco Bay-Delta Model (SFBM) to generate water-surface and current velocity data for the numerical model boundary conditions and the verification data sets.

c. The development of a higher resolution inset numerical model of the Alcatraz disposal area. This model was driven by the comprehensive model and used to establish water level and current velocity boundary conditions for use in the disposal model.

d. The use of the numerical model DIFID (Disposal From Instantaneous Dump) to simulate barge or hopper disposal of the dredged material. The model predicts the short-term fate (less than 1 hr) of disposed material, including the initial deposition pattern.

e. The use of the sediment transport model STUDH to simulate the fate of the disposed material using suspended sediment concentrations produced by the disposal model.

PART II: DESCRIPTION OF THE MODELS

Modeling Overview and Procedures

6. To calculate the short- and long-term transport of disposed sediment materials, hydrodynamic data are needed at many locations in the flow. Therefore, the first step in sediment modeling is the development of the necessary dynamic current field. Existing disposal models lack erosion and deposition features necessary for long-term predictions. Long-term sediment transport models lack disposal prediction capability. Therefore, a combination of models including a disposal model, a sediment transport model, and a hydrodynamic model were merged in this study. The models selected were DIFID, STUDH, and RMA-2V (Two-Dimensional Model for Open-Channel Flows). The latter two models are included in the TABS-2 modeling system supported by the US Army Corps of Engineers.

7. In addition to the family of numerical models, the physical model of San Francisco Bay was used to generate synoptic water-surface elevation and velocity data. These data would provide the necessary boundary condition information and the verification data sets for the numerical models.

The San Francisco Bay-Delta Model

8. The SFBM is a fixed-bed, distorted scale, tidal hydraulic model. This physical hydraulic model provides a means of reproducing on a manageable scale the hydrodynamic phenomena that occur throughout the large and complex estuarine system. The establishment of the similarity between model and prototype commonly makes use of laws of similitude expressed by a set of dimensionless numbers. These include the Froude, Reynolds, Weber, and Cauchy numbers, which are the ratios of inertial forces to the forces of gravity, viscosity, surface tension, and elasticity, respectively. Perfect similitude would require that each of these numbers be the same for model and prototype. Physical hydraulic models cannot be designed to provide similitude with respect to all forces, but are designed to simulate the dominant forces affecting the conditions being modeled. The scale is selected so that the remaining forces are negligible or do not cause fundamental dissimilarities in the processes of interest.

9. In the San Francisco Bay complex, the depth, surface slope, and other features of tidal flow are controlled by the joint effects of inertial and gravitational forces. The major hydraulic quantities vary according to the Froude number. For the SFBM, different model scales were chosen for horizontal and vertical lengths to reduce construction and operation time and cost as well as keep faithful reproduction of flows and permit measurements of the desired parameters with satisfactory accuracy. The effect of distortion on boundary roughness was reproduced during verification tests by the use of metal strips embedded in the model. These strips were adjusted to change the frictional resistance to obtain reproduction of the bay's tides, current, and salinities. The scaling ratios of model to prototype are as follows:

Characteristic	Scale Relations Model:Prototype
Horizontal length	1:1,000
Vertical length	1:100
Time	1:100
Velocity (horizontal)	1:10
Discharge	1:1,000,000
Salinity	1:1

10. The SFBM occupies an area of about 1 acre,* and is completely enclosed in a 128,500-sq-ft shelter to protect it from the weather and thus permit uninterrupted operation. The limits of the model, shown in Figure 2, encompass a portion of the Pacific Ocean extending 17 miles west of the Golden Gate, San Francisco Bay, San Pablo Bay, Suisun Bay, and all of the Sacramento-San Joaquin Delta east of Suisun Bay to the cities of Sacramento on the north, Stockton on the east, and Tracy to the south.

11. The model is equipped with the necessary appurtenances including freshwater and saltwater supply sumps, primary saltwater inflow and mixing pumps, computer-controlled tide generator capable of reproducing repetitive ocean tides by regulating two motorized gate valves, precise flowmeters to regulate major river inflows to the delta plus other inflow and withdrawal facilities, major pumping plant exports, and electrically operated one-way

* A table of factors for converting non-SI units of measurement to SI (metric) units is found on page 3.

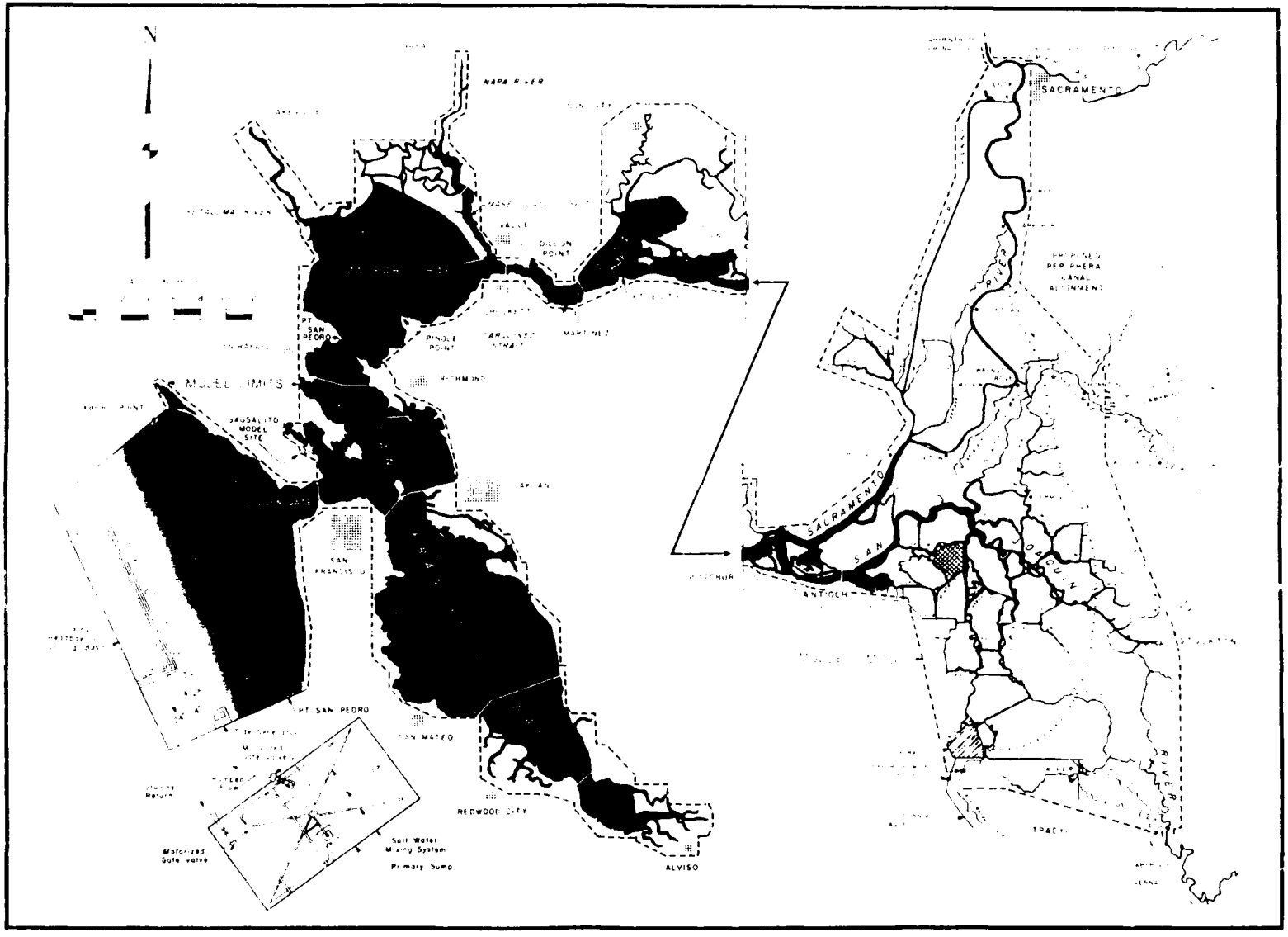

Figure 2. Limits of SFBM (from USAED, San Francisco, 1981)

head gates. The model represents the state of the art in model operation, real-time data acquisition using miniature sensors, data analysis, anc information storage/retrieval capability.

The TABS-2 Modeling System

12. The TABS-2 is a modular system composed of distinct computer programs linked together by preprocessors and postprocessors. Each of the major computer programs solves a particular type of problem: hydrodynamics (RMA-2V), sediment transport (STUDH), or water quality (RMA-4). These programs employ the finite element method to solve the governing equations. A brief description of RMA-2V and STUDH appears in Appendix A.

13. The major programs from the TABS-2 system used in this study are RMA-2V and STUDH. Along with a disposal model, DIFID, the three programs interact as shown in the following diagram:

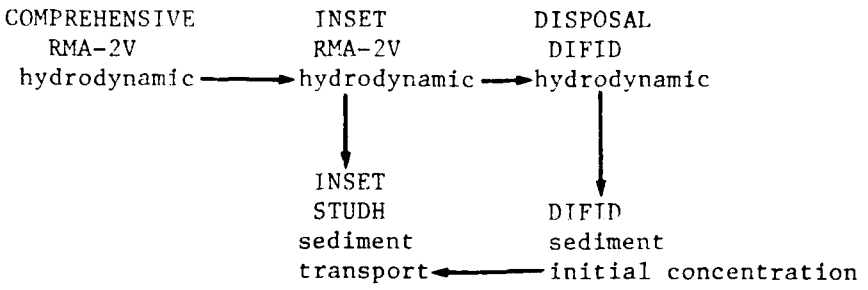

14. A summary of program codes used in this modeling effort and a flowchart of the code usage are presented in Table 1 and Figure 3, respectively. The procedures of model development and execution were followed as described in the TABS-2 user's manual (Thomas and McAnally 1985).

Hydrodynamic Model

15. RMA-2V is a finite element solution of the Reynolds form of the Navier-Stokes equations for turbulent flows. Friction is calculated with Manning's equation, and eddy viscosity coefficients are used to define turbulent exchange characteristics. A velocity form of the basic equation is used with side boundaries treated as either slip (parallel flow) or static (zero flow). The model recognizes computationally wet or dry elements and corrects

Table 1

Summary of Program Codes

Program	Description
GFGEN	Create geometric data file for use by models
EDGRG	Edit computational network interactively
CODE24	Process physical model data files for input to RMA-2V for use as time-dependent boundary conditions
RMA-2V	Compute two-dimensional vertically averaged flows and water levels
JOBSTRM	Compute boundary conditions for an inset computational network from results of a larger network model run
VPLOT	Produce vector plots of RMA-2V velocity results
POSTHYD	Analyze results of an RMA-2V run and plot time-histories
DIFID	Compute suspended sediment concentrations and initial deposition on the bottom of material released into the water column from a dredged material disposal operation
ENGMET	Translate RMA-2V output from non-SI (English) units to SI (metric) units for use by STUDH
STUDH	Compute two-dimensional vertically averaged transport, erosion, and deposition of sediments
SEDGRAF	Produce factor map of STUDH results

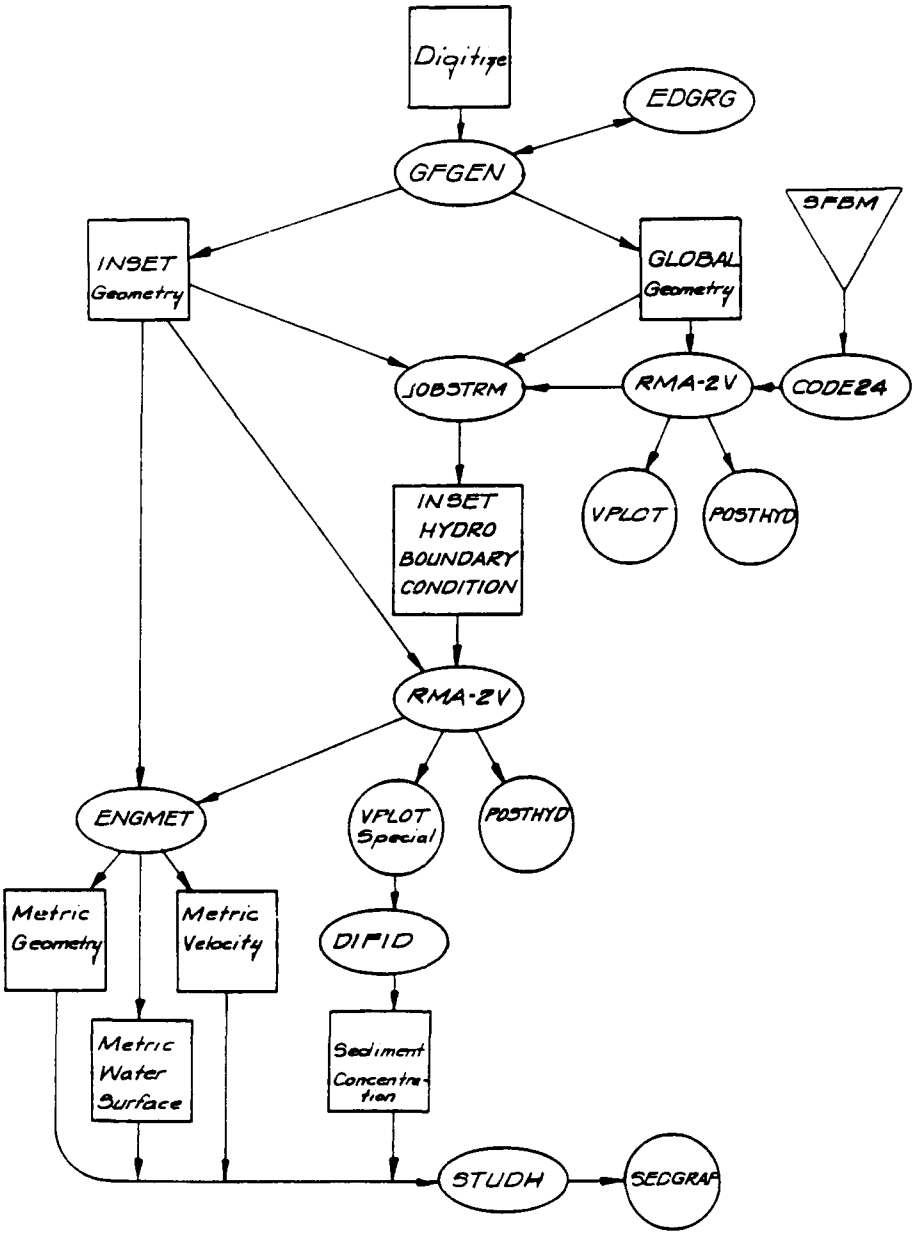

Figure 3. Flowchart of programs

the mesh accordingly. Boundary conditions may be water-surface elevations, velocities, or discharges and may occur inside the mesh as well as along the outer boundaries.

Comprehensive mesh

16. Model limits. The comprehensive or global model was established as extending from 7 nautical miles west of the mouth of San Francisco Bay to Carquinez Strait between San Pablo and Suisun bays. A mesh was developed consisting of 1,580 quadrilateral elements with 5,000 nodes. The bathymetric contours of the bay were major factors in the location, shape, and size of the elements. The boundaries were represented by curved element sides, and the model included the five islands of Alcatraz, Angel, Brooks, and Treasure/Yerba Buena and lower San Pablo Bay.

17. Bathymetry. Bathymetric data input to the model were derived from the following 1:40,000-scale National Ocean Survey charts:

Chart No.	Location	Date
18651	San Francisco Bay--Southern Part	1978
18649	Entrance to San Francisco Bay	1985
18654	San Pablo Bay	1983
18656	Suisun Bay	1983

18. An x-coordinate, y-coordinate, and z-value (bed elevation) were assigned to each of the 5,000 nodes during the digitizing process and stored in a computer file for further use and modification. The vertical datum was mean lower low water (mllw). Element types were established, and eddy viscosity (turbulent exchange coefficient) and Manning's n (bottom friction) values were assigned to each element type.

19. The network generation program GFGEN was used to create a geometry and finite element computational mesh file for input to the TABS-2 modeling system. A utility program, EDGRG, was used to interactively edit the computational mesh. With EDGRG, curved boundaries can be fitted and nodes and elements of the mesh can be moved, added, or deleted. These changes can be saved as a permanent file.

20. Boundary conditions. If no boundary condition is specified at a node, the program computes velocity x- and y-components and the water depth at that node. For the nodes along solid boundaries (land/water interface), slip flows parallel to the boundary were specified. A head specification (water-surface elevation) was assigned to the Pacific Ocean boundary nodes. These

nodes had a water-surface elevation specified at each time-step. The freshwater inflow boundaries at Benicia, Mare Island, and South Bay had velocity specifications (Figure 4).

21. The input data for the boundary conditions of the numerical model were supplied by the SFBM (USAED, San Francisco, in preparation). Four conditions were simulated in the physical model:

a. Nineteen-year mean ocean tide with low freshwater delta outflow (4,400 cfs).

b. Nineteen-year mean ocean tide with high freshwater delta outflow (40,000 cfs).

c. Spring ocean tide with low freshwater delta outflow.

d. Spring ocean tide with high freshwater delta outflow.

Synoptic data were taken at 10 tide and 36 velocity stations under each of the four test conditions. These data were used to provide boundary conditions and verify the numerical hydrodynamic model.

22. Conversion of the physical model data as input to the RMA-2V hydrodynamic model for use as time-dependent boundary conditions was performed by the utility code CODE24. CODE24 reads files containing physical model velocities and water-surface elevations and produces a boundary control update file for RMA-2V. This file contains time-varying water-surface elevations and x- and y-direction velocity components.

23. Time-step. The time-step used for the numerical simulations was the same as that used for data collection on the physical model. The 24.84-hr lunar day was divided into 40 equal parts producing a time-step of 37.26 minutes. The same time increment was used to make direct physical model/numerical model data comparisons.

24. RMA-2V output. The output files from an RMA-2V run consist of a water-surface elevation and velocity file in binary format, a binary hot-start file (which can be used to start a continuation run), and a line printer ASCII output. No graphics are produced by RMA-2V. Instead the output file is ready for use by utility programs, which prepare velocity vector plots, time-history plots, contours, or other plotted outputs.

Inset mesh

25. An area containing Alcatraz Island and the Alcatraz dredged material disposal site was chosen to become the higher resolution "inset" mesh (Figure 5). The disposal area, which consisted of one element in the global

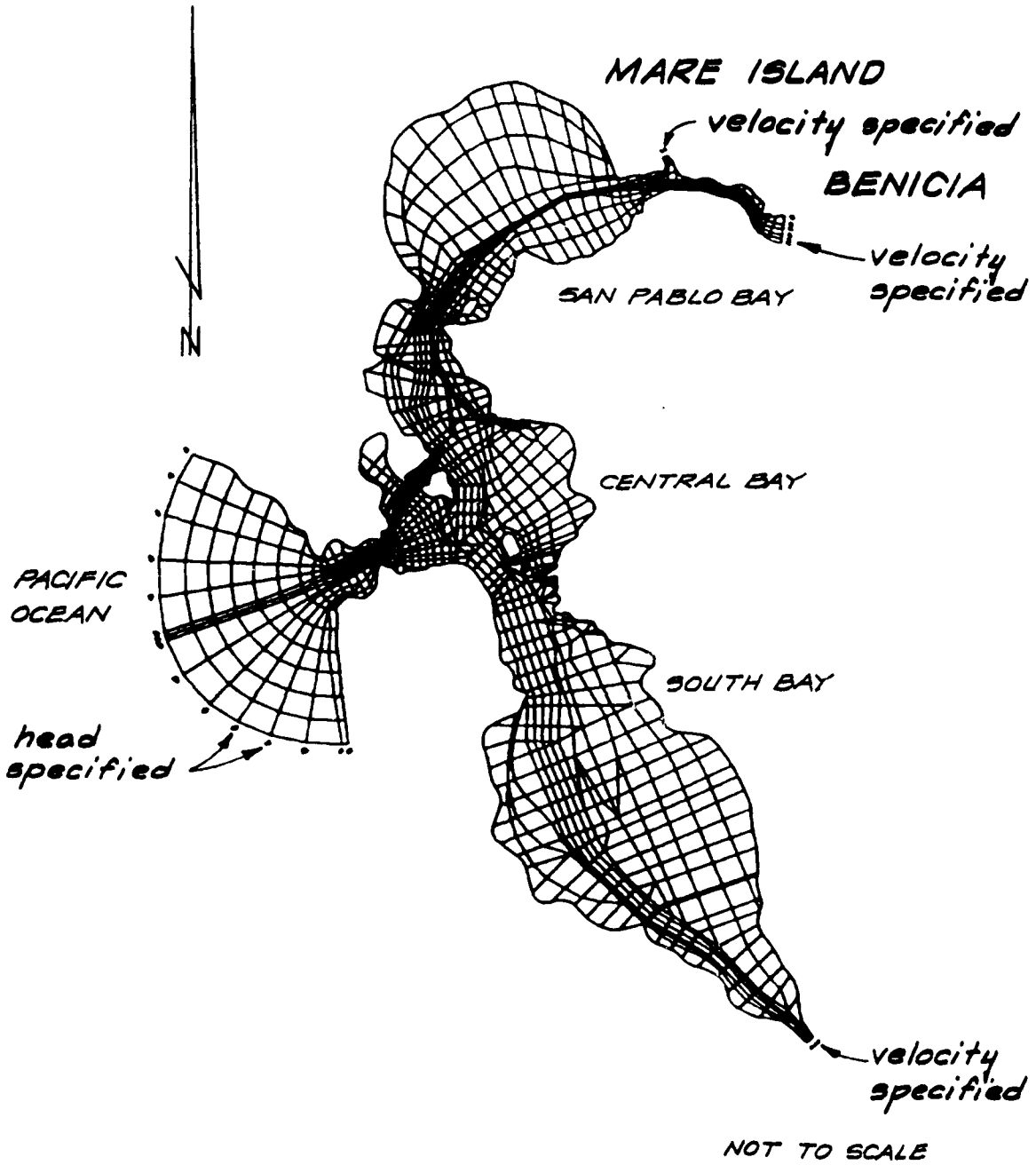

Figure 4. San Francisco Bay global mesh with boundary specifications

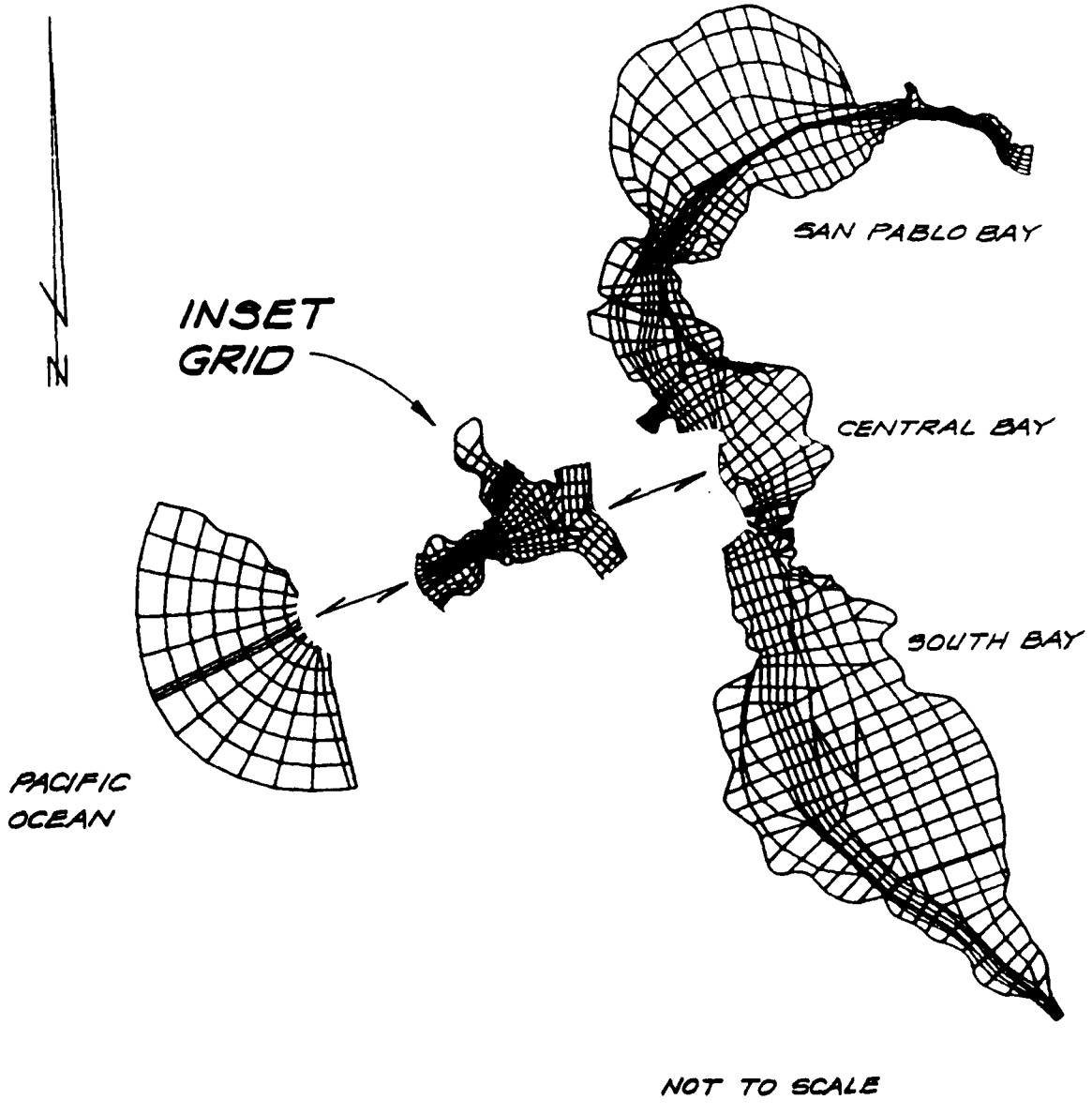

Figure 5. San Francisco Bay global mesh with inset grid indicated

mesh, was changed to 25 small higher resolution elements in the inset mesh. All elements in the lower Central Bay and Golden Gate areas were reduced in size to increase resolution in the area affected by the disposal operations. The digitized mesh contained x- and y-coordinates and bed elevations for 584 elements and 1,802 nodes. An interface program, JOBSTRM, was used to create an inset mesh boundary condition file for RMA-2V using output files from previous runs of the program on the global mesh. Water-surface elevations were specified at the ocean boundary, and velocity specifications were assigned to the remaining water boundaries (Figure 6).

Disposal Model

26. The model used for the Alcatraz disposal site simulation was DIFID. This numerical model accounts for the physical processes that determine the short-term fate of dredged material disposed at an open-water site. Disposal phases include convective descent, dynamic collapse and spreading, and long-term diffusion. The long-term diffusion phase in DIFID assumes a uniform current field, which is unrealistic for the Alcatraz disposal site. Therefore, long-term diffusion calculations were performed using the STUDH sediment transport model. Output from DIFID includes an estimate of suspended sediment concentration and the initial deposition of material on the bottom. An explanation of the theoretical basis of DIFID (Trawle and Johnson 1986a) can be found in Appendix B. Grid development and model execution were performed according to Johnson (in preparation).

Model limits

27. The DIFID model requires a grid of uniformly sized square cells. Therefore, a grid of 17 by 39 cells, each cell 400 ft by 400 ft, was used to represent the area identified in Figure 7. The input file contained a depth for each grid point and information pertaining to the disposal site (ambient current velocities, vertical mixing coefficients, and vertical water density gradient), the character of the dredged material (bulk density, sediment composition, and particle velocities), and the disposal operation (barge position on grid, vessel dimensions and velocity, and volume of material to be disposed).

Hydrodynamic input

28. Using the binary output files from the inset mesh RMA-2V

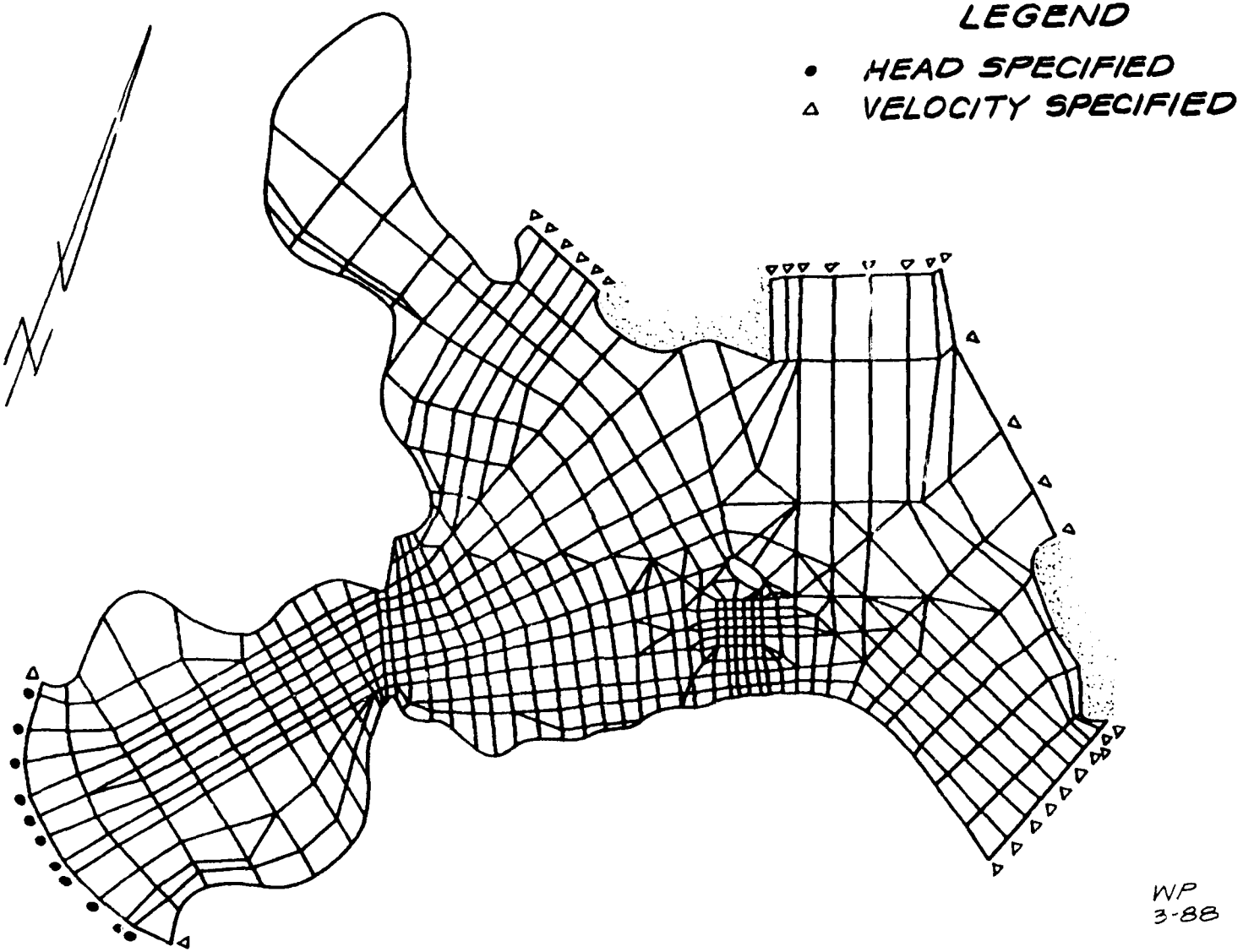

Figure 6. Alcatraz inset mesh with boundary condition nodes

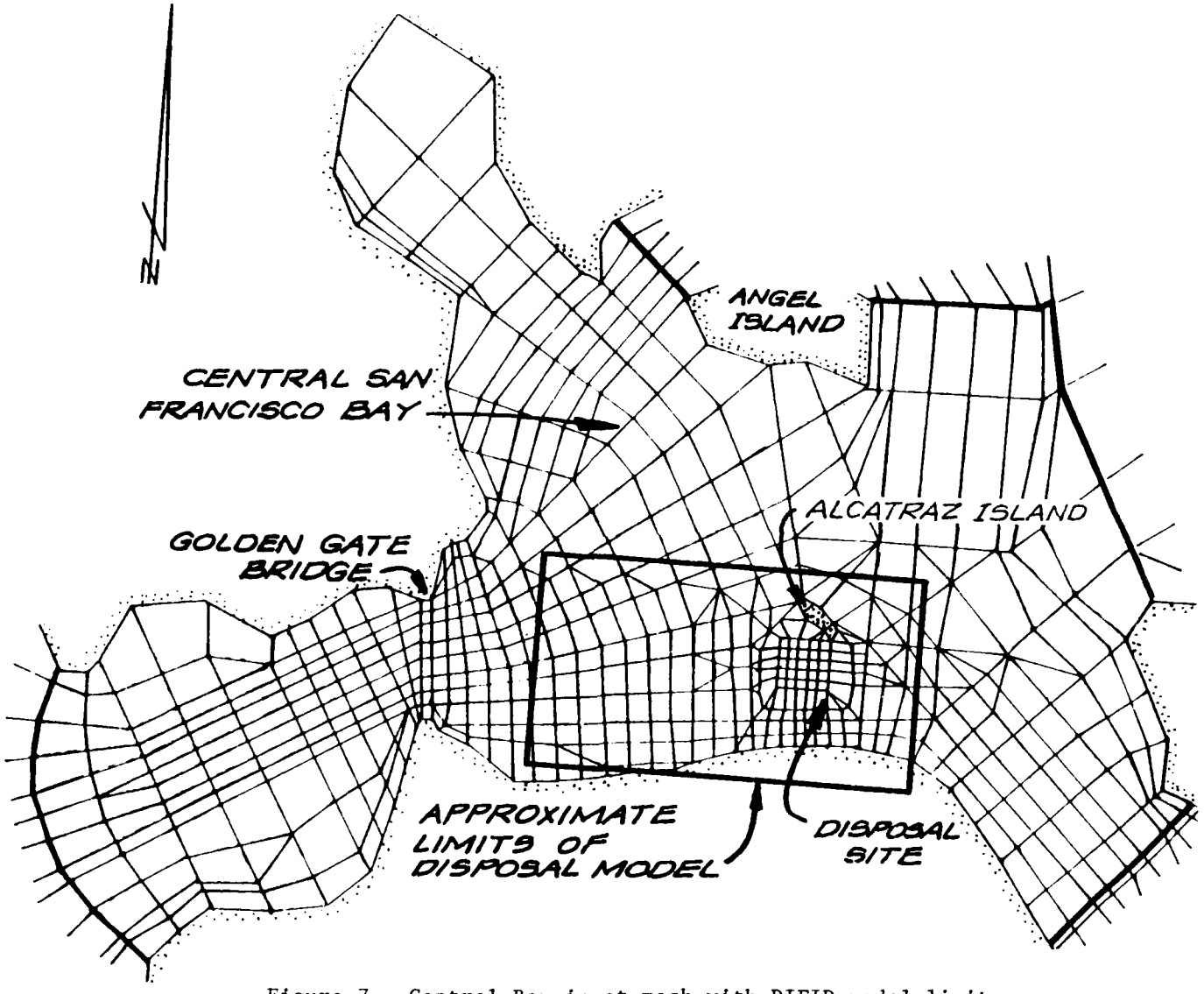

Figure 7. Central Bay inset mesh with DIFID model limits

simulations, the TABS-2 program VPLOT was used to create a special velocity output file that was interpolated onto a rectangular grid. This rectangular grid velocity file, which contained x- and y-location coordinates and x- and y-velocity components, was used to establish the velocity field for the disposal model. The DIFID model was run under conditions of maximum flood and ebb velocities.

DIFID output

29. The user-specified output from these simulations was in the form of a computer printout that listed water column suspended sediment concentrations and bottom accumulation for each solid fraction identified in the input file, at the designated depths and times following the disposal operation.

Sediment Transport Model

30. The sediment transport model in the TABS-2 system is STUDH. This model solves the convection-diffusion transport equation with bed source terms. These terms are structured for either sand or cohesive sediments. The Ackers-White (1973) procedure is used to calculate a sediment transport potential for the sands from which the actual transport is calculated based on the availability. Clay erosion is treated as described in Ariathurai, MacArthur, and Krone (1977), and the deposition of clay uses Krone's (1962) equations. Deposited material forms layers, and bookkeeping within the STUDH code allows up to 10 layers at each node for maintaining separate material types, deposited thickness, density, and age. The code uses the same mesh as RMA-2V. This model was used to predict suspended sediment transport resulting from sediment introduction into the water column during the disposal operation.

Input

31. Input information necessary for STUDH includes the geometry file from GFGEN, velocity and water-surface files from RMA-2V, and the run-control file containing suspended sediment characteristics and concentration (results from the disposal operation plus any background concentrations that might be present). The inset mesh geometry was used, and with the use of the utility program ENGMET, the GFGEN and RMA-2V files were converted from non-SI to SI (metric) units as required for STUDH.

STUDH output

32. The binary output file from STUDH consists of sediment

concentration, velocity, water depth, and bed changes at designated nodes. No graphics are produced by STUDH; however the output file is ready for use by utility programs which prepare plots of sediment transport and new bottom contours.

Model Integration

33. As can be seen from the preceding discussion, utility programs within the TABS-2 system enable output files from one program to become input to other programs in the system. Program output is in a format that is usable by a set of plot programs to display the data in several formats. The same mesh can be used by the hydrodynamic and the sedimentation transport codes, saving time and confusion. Utility programs are available to edit and change the mesh. This is economical for small changes; however, in this study, it was easier and less time-consuming to redigitize and renumber the inset mesh.

PART III: VERIFICATION AND APPLICATION OF THE MODELS

Physical Model Verification

34. The verification report of the San Francisco Bay physical model (USAED, San Francisco, 1963) indicated that the model could reproduce a prototype mean tide (21-22 September 1956) with good results. Maximum error in elevation in model reproduction at 23 gages throughout the bay was 0.4 ft prototype, with the model amplitudes being slightly less than those of the prototype. The verification procedure indicated that local model velocities may vary up to 20 percent from those in the prototype, the model velocities tending to be generally higher than those in the prototype. Additional prototype to model comparisons made in 1976 (USAED, San Francisco, 1976) were similar.

Hydrodynamic Model Verification

35. Verification of the RMA-2V model consisted of several test runs to adjust the boundary conditions and internal coefficients so the numerical model would reproduce water-surface elevations and current velocities supplied by the SFBM. Verification of the model started with static leak tests to ensure the integrity of the numerical mesh. Next, steady state and dynamic conditions were imposed at the boundaries. Progressive sophistication of these tests included adjusting one parameter at a time to determine the effect on the model. This iterative process of adjustments resulted in the final global mesh with designated internal coefficients and dynamic boundary conditions.

Test conditions

36. Two sets of physical model data were used to verify the hydrodynamic model. First a 19-year mean tide was generated at the ocean tide generator to produce a mixed tide with extremes of 2.3, 5.8, 0.0, and 4.6 ft mllw at sta 8, Presidio, Golden Gate. The delta net outflow was maintained at 4,400 cfs. After all adjustments were made and the RMA-2V model was satisfactorially reproducing the mean tide physical model data, a second data set was used. These data were a simulation of a 28-29 December 1955 spring tide with extreme values of 3.0, 7.2, -1.2, and 4.9 ft mllw at sta 8 with the same 4,400-cfs delta net outflow.

Model coefficients

37. The bay was divided into four major eddy viscosity coefficient zones. Each zone had four to five different Manning's n values depending on the water depth and the size of the element, with greater roughness (0.03) for shallow areas and less roughness (0.015) for deep areas. Eddy viscosity coefficients were assigned according to the turbulence characteristics of the region and ranged from 200 to 1,000 lb-sec/ft^2.

38. Physical model data were put into the format compatible with the TABS-2 system requirements. The velocity boundary specifications were adjusted in magnitude and direction when necessary to create entrance conditions needed to produce the desired results inside the mesh. Similarly, the physical model tide data at the ocean tide sta 0 was adjusted 1 hr in timing to reproduce the desired tide at the tide stations inside the global mesh.

39. Velocity output from RMA-2V is vertically averaged. Before comparisons could be made, the physical model data were also vertically averaged. Physical model stations that reported only middepth values were unaffected, and the data were used as reported. For stations that reported surface (5 ft below mllw) and bottom (5-10 ft above bed) velocity values, an average of the two was used. Sta 1 at the Golden Gate reported data from the surface and middepth, and a value equal to 85 percent of the surface velocity was used.

Global mesh verification

40. The numerical simulation was 30 hr with the data from the last 25 hr plotted. The lead-in 5 hr was spin-up time and was used as a hot-start input file for the final run. Ten tide and thirteen velocity stations were chosen for RMA-2V and physical model comparisons (Figure . Plates 1-7 are tide and velocity station comparison plots for the mean tide, 4,400-cfs net delta outflow simulation; and Plates 8-14 are the comparisons for the spring tide, 4,400-cfs net delta outflow conditions.

41. Tide comparisons for mean tide conditions were good. Phase differences were less than one 37-min time-step, and amplitude values compared favorably. The tide planes (means) of RMA-2V values were 0.10 ft and 0.20 ft lower at the South Bay sta 2 and Carquinez Strait sta 20, respectively. All interior tide stations had good tide plane agreement.

42. Comparisons of RMA-2V versus physical model velocity values were reasonable. RMA-2V velocity amplitudes tended to be lower than the physical model at most station. Sta 1-4B in both the numerical and physical models

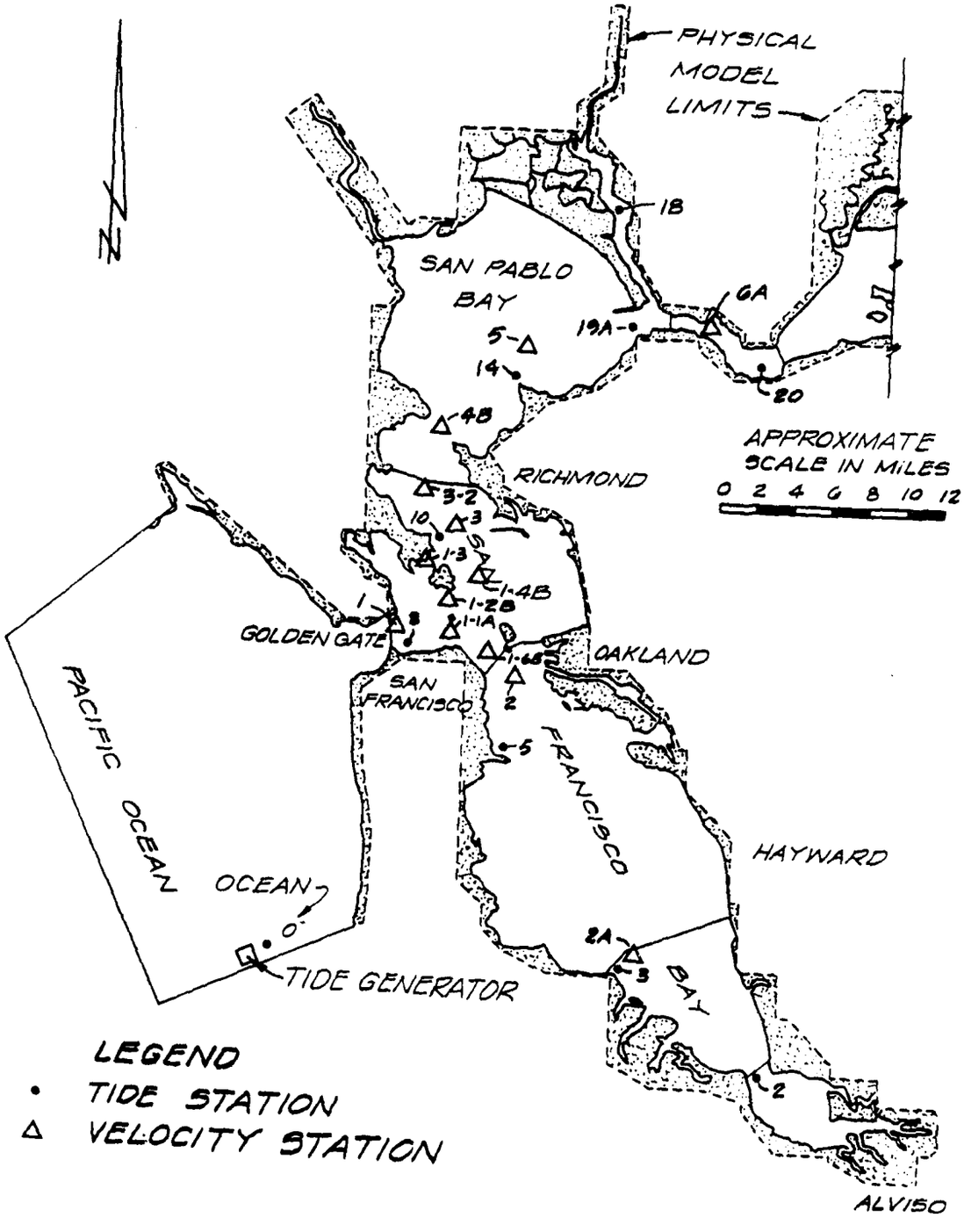

Figure 8. San Francisco Bay area with physical model limits and station locations

displayed the same unusual flattened velocity characteristics.

43. Using the same geometry, eddy viscosity coefficients, Manning's n roughness values, and net delta outflow, a model simulation of the spring tide was run. The same tide and velocity stations were examined for comparisons. All RMA-2V tide and velocity stations compared favorably with the physical model data and displayed the same characteristics as seen in the mean tide data comparisons.

Inset mesh verification

44. The turbulence and roughness coefficients used in the inset mesh were adjusted to be compatible with the smaller size of the new elements. Once this was done, a simulation of the mean tide, 4,400-cfs net delta outflow condition was run. Comparisons of tide and velocity data of RMA-2V inset mesh, RMA-2V global mesh, and physical model were good. The comparisons of tide and velocity data for the inset and global mesh stations showed no general pattern of variation, phase agreement was good, and tide and velocity amplitudes differed from 0 to 0.5 ft (tide) and 0 to 0.5 fps (velocity). When the inset mesh and physical model data were compared, the RMA-2V velocity values again tended to be slightly lower than the physical model values. However, the inset mesh velocity comparisons were slightly better than global mesh versus physical model comparisons. This was due to the higher resolution of the smaller inset mesh. Plate 15 is the plotted data from selected stations of inset mesh versus global mesh, and Plate 16 shows data for the inset mesh versus the physical model.

Results

45. The RMA-2V hydrodynamic model was verified to the two sets of the physical model data. Both the global and the high-resolution inset mesh reproduced the tides and velocities of the SFBM with reasonable accuracy and repeatability.

Disposal Model Validation

46. In this application the disposal model, DIFID, was not verified to field or other model data. It has, however, been shown to provide reasonable results at this site compared to field experience and good comparison to field data at other sites (Trawle and Johnson 1986b). Thus the disposal model is considered to be validated (well grounded on principles and generally capable

of reproducing observed behavior) but not verified (compared directly to San Francisco Bay/Alcatraz site field data).

Test conditions

47. The disposal simulation consisted of 1,000 cu yd of hydraulically dredged material, primarily silt-clays, being disposed from a stationary barge in the Alcatraz dredged material disposal site. Sediment characteristics and barge location were similar to the information presented in Phase II of the Alcatraz disposal site survey (Science Applications International Corporation (SAIC) 1987).

48. Two disposal operations were simulated, one at maximum ebb and the other at maximum flood velocities. The clay-silt material that did not reach bottom but remained in suspension was tabulated at four depths, 10, 30, 50, and 70 ft, at several time intervals after the disposal operation.

49. The DIFID model was run using a velocity field from the RMA-2V mean tide simulation (Figure 9). A special version of VPLOT converted the velocity vectors from the nodes and midsides of the elements in the inset mesh to a regular mesh of the size and spacing designed (Figure 10).

Model coefficients

50. There are 14 coefficients in DIFID that require input values. Default values based on previous laboratory and field experiments are included in the model. Computer experimentation such as presented by Johnson and Holliday (1978) has shown that model results appear to be fairly insensitive to many of the coefficients. Therefore, the model default values were used for these simulations.

Disposal model results

51. The suspended sediment plume predicted by DIFID displayed similar characteristics to the SAIC (1987) Phase II study in that it did not persist beyond 10-15 min, had comparable flood and ebb plume direction and distance of travel features, and had no significant north/south dispersion. Figure 11 is a sample of the printed output from the DIFID ebb velocity simulation showing silt-clay concentrations 40 ft below the water surface, 540 sec (9 min) after the disposal. Alcatraz Island (land) and the location of the disposal barge are shown on the grid.

Discussion of results

52. The field data available in the SAIC (1987) report indicate the disposal model reasonably simulated the disposal process in the Alcatraz site.

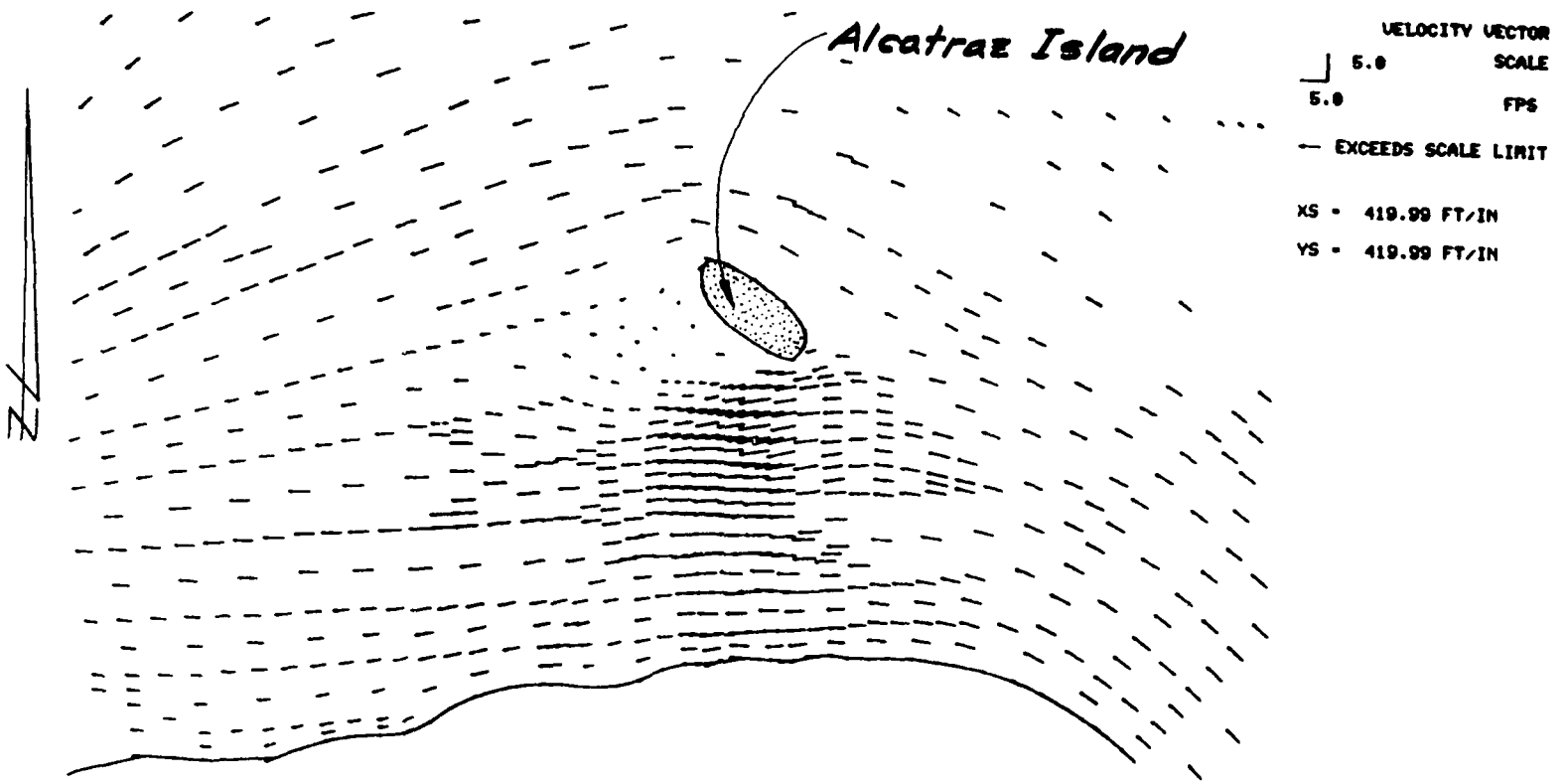

Figure 9. Alcatraz Island, RMA-2V velocity vectors at maximum ebb

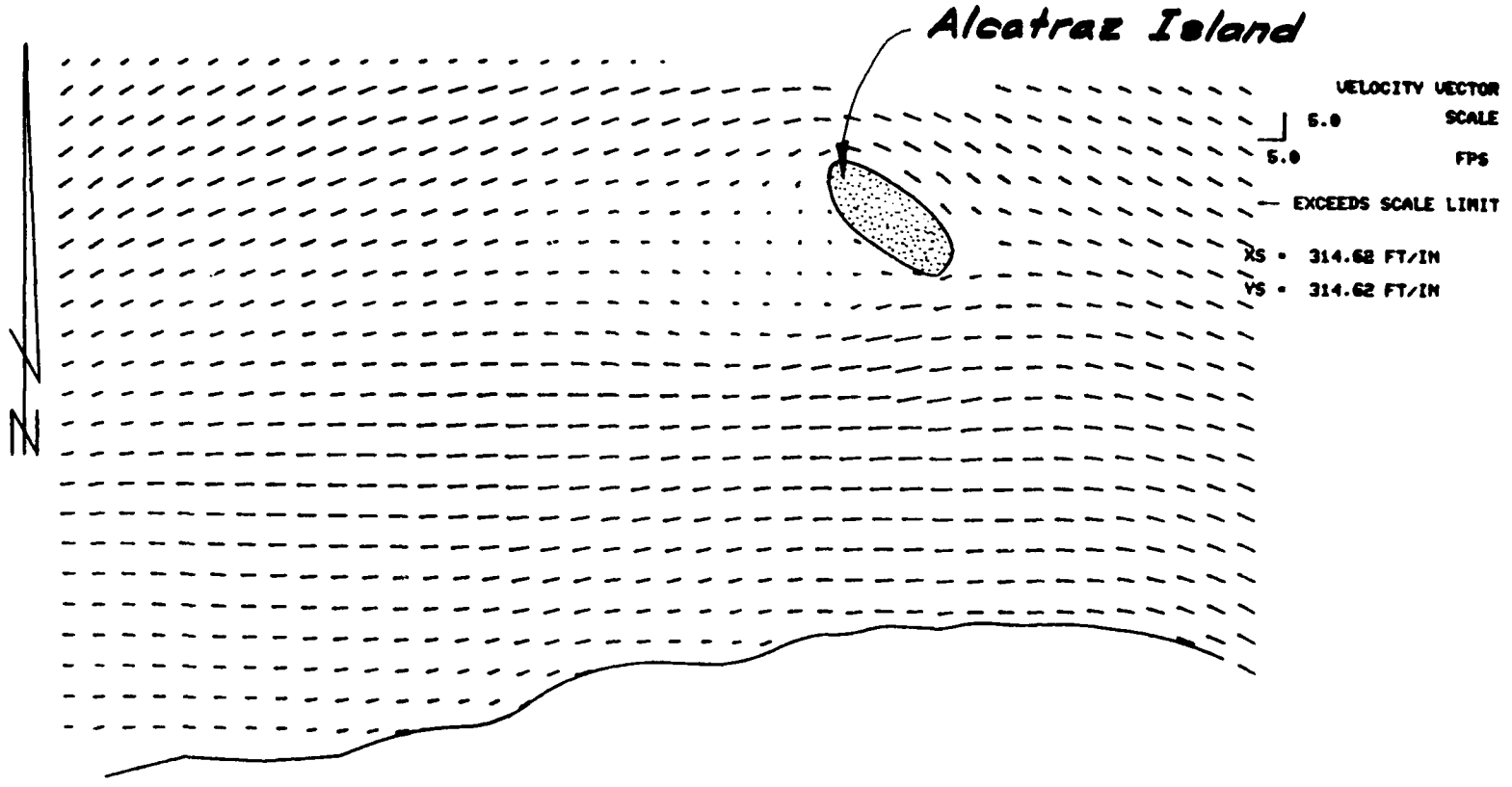

Figure 10. Alcatraz Island, VPLOT conversion of RMA - 2V velocity vectors at maximum ebb

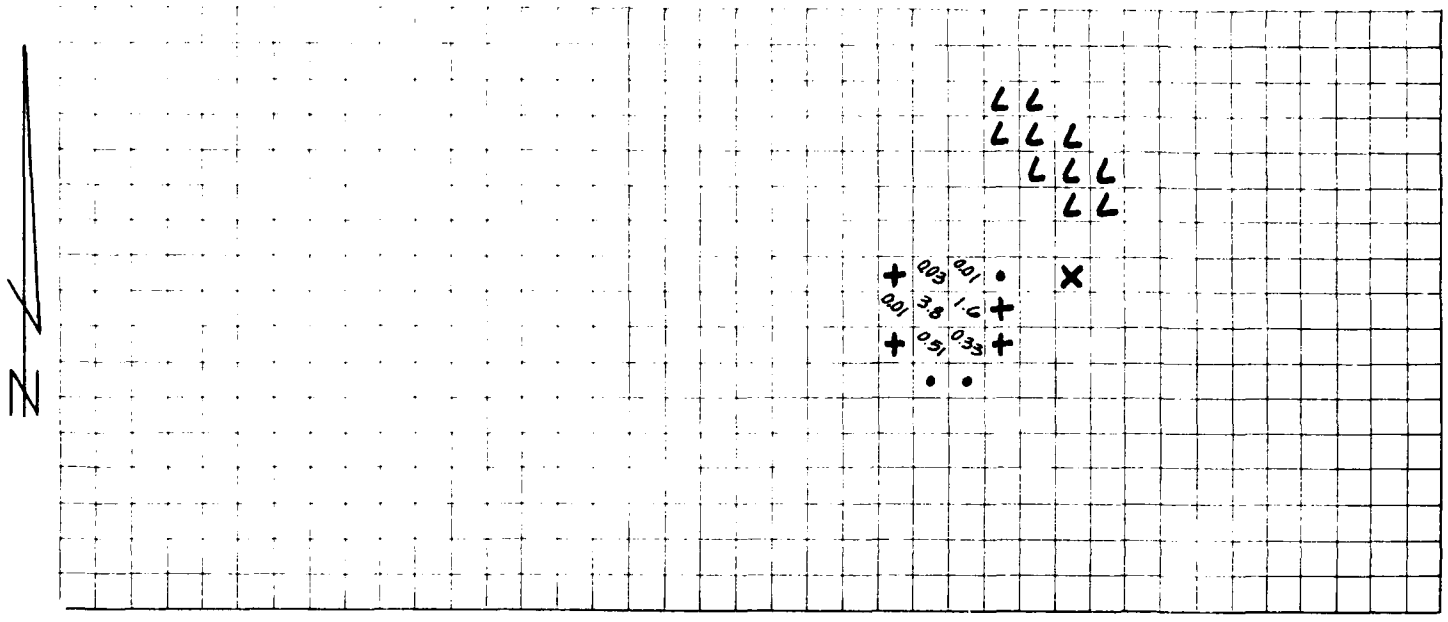

EBB VELOCITY SIMULATION

NOT TO SCALE

+ = < 0.01 mg/ℓ* L = land

• = < 0.001 mg/ℓ* X = barge location

* concentrations above background

Note: multiply values by 0.1000E-04

Figure 11. Sample DIFID output, summary of silt-clay distribution after 540 sec, 40 ft below water surface

The default model coefficients used in DIFID could be made more site specific in the future as a better understanding of sediment behavior at the Alcatraz site is achieved.

53. The purpose of the simulation was to produce disposal-related suspended sediment concentrations as input into the TABS-2 sediment transport model STUDH. This was achieved by averaging the suspended sediment concentrations in the water column in each cell of the DIFID grid and assigning these values to the comparable inset mesh nodes and midsides.

Application of Sediment Transport Model

54. The sediment transport model STUDH was used to trace the sediment movement through the system. As in the case of the disposal model, no field data were available to verify STUDH. Normally in the verification process, the model coefficients are adjusted until the model produces results similar to conditions observed in the prototype. In the absence of verification data, the coefficients used were realistic estimates of the general prototype and sediment characteristics found in the Alcatraz disposal area.

Test conditions

55. The inset mesh geometry was used with the RMA-2V hydrodynamic output data from the mean tide, low flow simulation. Along with the run control file, these data, converted into metric units, are necessary input to run STUDH. Sediment concentrations (from DIFID) assigned to designated inset mesh nodes and the sediment transport coefficients were included in the run control file. The sediment concentrations from the disposal at maximum ebb velocity were used, and seven time-steps (two before and four after maximum ebb velocity for a total of 4.3 hr) were simulated.

Model coefficients

56. The primary function of this simulation was to evaluate the use of STUDH in the application of tracing suspended sediment movement in the system. Therefore, all terms relating to bed deposition and erosion were turned off. Only required coefficients were used. A fluid temperature of 20° C and a fluid density of 1,025 kg/cu m were also specified.

57. The initial runs of STUDH were unstable with oscillations in the sediment concentration results. Adjustments were made one at a time to the length of the time-step (37 min, 18 min, and 4 min); x- and y-diffusion

coefficients (EX = 25 sq m/sec, EY = 10 sq m/sec; and EX = 50 sq m/sec, EY = 25 sq m/sec); and Crank-Nicholson THETA values (0.5, 0.67, 0.9, and 1.0). Simulations were also made with and without background and boundary sediment concentrations. The adjustment that made the most difference and improved the stability of the model was the Crank-Nicholson THETA value. With a value of 1.0, the oscillations were quelled and the solutions were stable. The simulation described in this report was run with the following: time-step of 2,235.6 sec (37 min); diffusion coefficients of EX 25 sq m/sec, EY 10 sq m/sec; Crank-Nicholson THETA of 1.0; and a background and boundary sediment concentration of 20 mg/ℓ.

Transport model results

58. The STUDH results, although unverified, were promising and showed a reasonable progression of suspended sediment out of the disposal site. The results were more stable when the simulation was run with a background concentration, the solution ending at the background value. When no background was specified, the solution continued to approach zero but never quite reached it, sometimes going to small negative numbers. Plates 17-19 are plots of the predicted suspended sediment at 37-min time-steps for 3.73 hr after the disposal operation, which took place during the time of ebb current velocity.

Results

59. It has been demonstrated that STUDH can be used to trace the movement of suspended sediment from the Alcatraz disposal site through the Central Bay system. Additional refinement and prototype data are needed to adjust the model coefficients to be more representative of the transport process.

60. In the absence of verification field data, the modelers must rely on their experience and familiarity with both the San Francisco Bay and the TABS-2 modeling systems to establish the modeling coefficients that best represent the prototype processes.

PART IV: CONCLUSIONS

61. The use of the San Francisco Bay-Delta (SFBM) physical model and the TABS-2 modeling system has produced an interrelated set of models that can simulate and address many hydrodynamic, circulation, and suspended sediment transport questions of most portions of the San Francisco Bay system.

62. The RMA-2V hydrodynamic model of both the comprehensive and the more detailed inset meshes have been verified to data produced in the SFBM physical model.

63. The disposal model, DIFID, produced suspended sediment results similar to field data and established a realistic suspended sediment cloud that might be produced by a dredged material disposal operation in the Alcatraz disposal site during the time following maximum ebb current velocities.

64. The coupling of the geometry, hydrodynamics, and sediment input in the transport model, STUDH, produced a reasonable sediment transport pattern out of the disposal site. Specific clouds of sediment concentrations could be identified and monitored as they travelled and dispersed through the system.

65. The modeling system has its capabilities and applications. However, the results are just reasonable simulations, not fully verified ones. Each of the numerical models, RMA-2V, DIFID, and STUDH, has individual capabilities and limitations, the greatest of which is the two-dimensional approximation of a three-dimensional phenomenon. The vertically averaged velocities and sediment fields will mask two-layer flow and other three-dimensional processes. Even with this simplification, the model results are useful in estimating the short- and long-term fates of sediments released during a disposal operation.

REFERENCES

Ackers, P., and White, W. R. 1973 (Nov). "Sediment Transport: New Approach and Analysis," Journal, Hydraulics Division, American Society of Civil Engineers, No. HY-11

Ariathurai, R., MacArthur, R. D., and Krone, R. C. 1977 (Oct). "Mathematical Model of Estuarial Sediment Transport," Technical Report D-77-12, US Army Engineer Waterways Experiment Station, Vicksburg, MS.

Johnson, B. H. "User's Guide For Models of Dredged Material Disposal in Open Water" (in preparation), US Army Engineer Waterways Experiment Station, Vicksburg, Miss.

Johnson, B. H., and Holliday, B. W. 1978 (Aug). "Evaluation and Calibration of Tetra Tech Dredged Material Disposal Models Based on Field Data," Technical Report D-78-47, US Army Engineer Waterways Experiment Station, Vicksburg, MS.

Krone, R. B. 1962. "Flume Studies of Transport of Sediment in Estuarial Shoaling Processes," Final Report. Hydraulics Engineering Research Laboratory, University of California, Berkeley, CA.

Science Applications International Corporation. 1987 (May). "Alcatraz Disposal Site Survey, Phase II, Richmond Channel Hopper Dredge Operation, Technical Report," SAIC Report 87/7517-144, Ocean Science & Technology Division, SAIC, Newport, RI.

Thomas, W. A., and McAnally, W. H., Jr. 1985 (Aug). "User's Manual for the Generalized Computer Program System, Open-Channel Flow and Sedimentation, TABS-2, Main Text and Appendices A through O," Instruction Report HL-85-1, US Army Engineer Waterways Experiment Station, Vicksburg, MS.

Trawle, M. J., and Johnson, B. H. 1986a (Mar). "Alcatraz Disposal Site Investigation," Miscellaneous Paper HL-86-1, US Army Engineer Waterways Experiment Station, Vicksburg, MS.

_____. 1986b (Aug). "Puget Sound Generic Dredged Material Disposal Alternatives," Miscellaneous Paper HL-86-5, US Army Engineer Waterways Experiment Station, Vicksburg, MS.

US Army Engineer District, San Francisco. 1963 (Mar). "Comprehensive Survey of San Francisco Bay and Tributaries, California; Appendix H, Hydraulic Model Studies; Volume I, Text and Figures; and Volume II, Plates: Verification and Tests of Barriers, to the Technical Report on San Francisco Bay Barriers," San Francisco, CA.

_____. 1976 (Jun). "San Francisco Bay and Sacramento, San Joaquin Delta Water Quality and Waste Disposal Investigation, San Francisco Bay; Model Verification and Results of Sensitivity Tests," Delta Model Technical Memorandum No. 1, San Francisco, CA.

_____. 1981 (Dec). "User's Guide for the San Francisco Bay-Delta Tidal Hydraulic Model," San Francisco, CA.

_____. "Physical Model Hydraulic/Salinity Sampling Program for WES Verification of TABS-2 Numerical Model" (in preparation), San Francisco, CA.

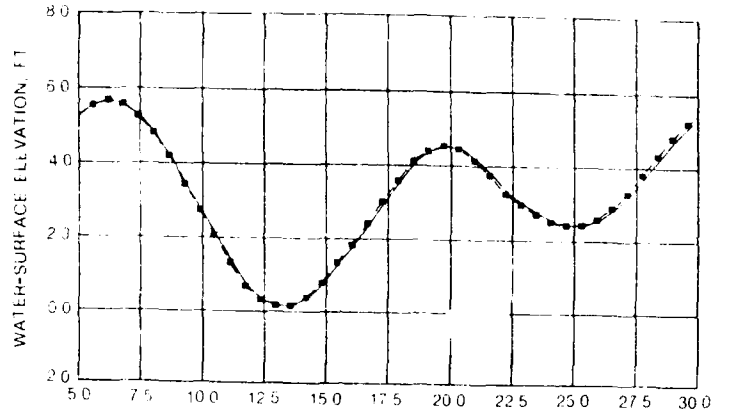

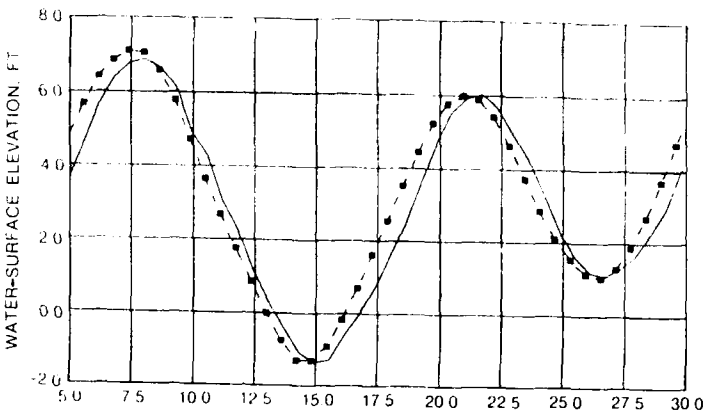

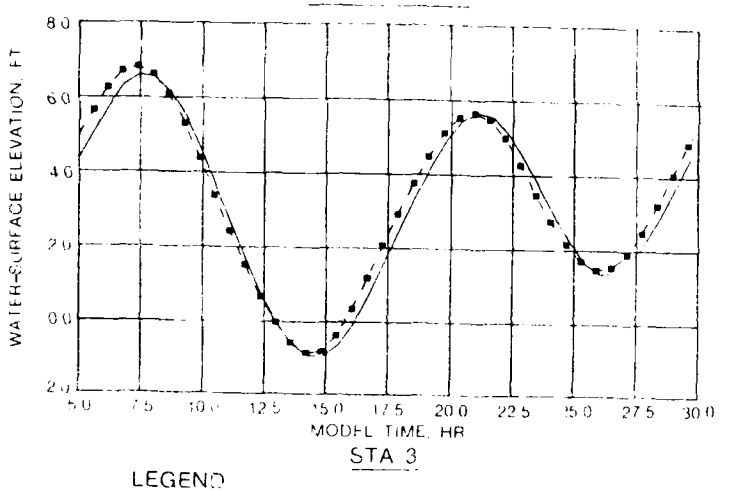

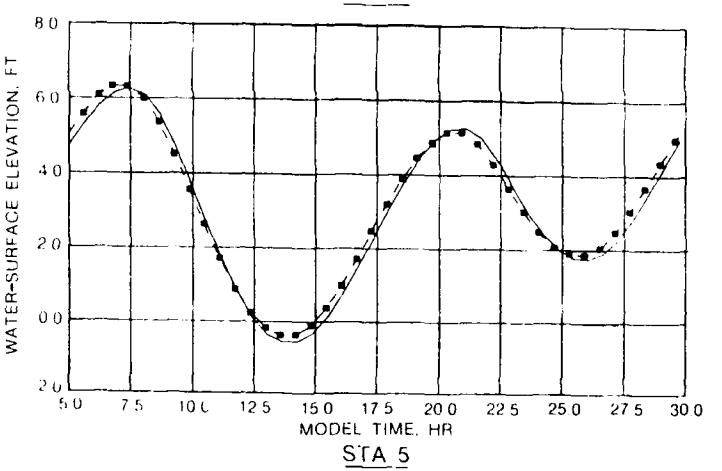

LEGEND

RMA-2V

PHYSICAL MODEL

MEAN TIDE DATA

RMA-2V VERSUS PHYSICAL MODEL

OCEAN AND SOUTH BAY

PLATE 1

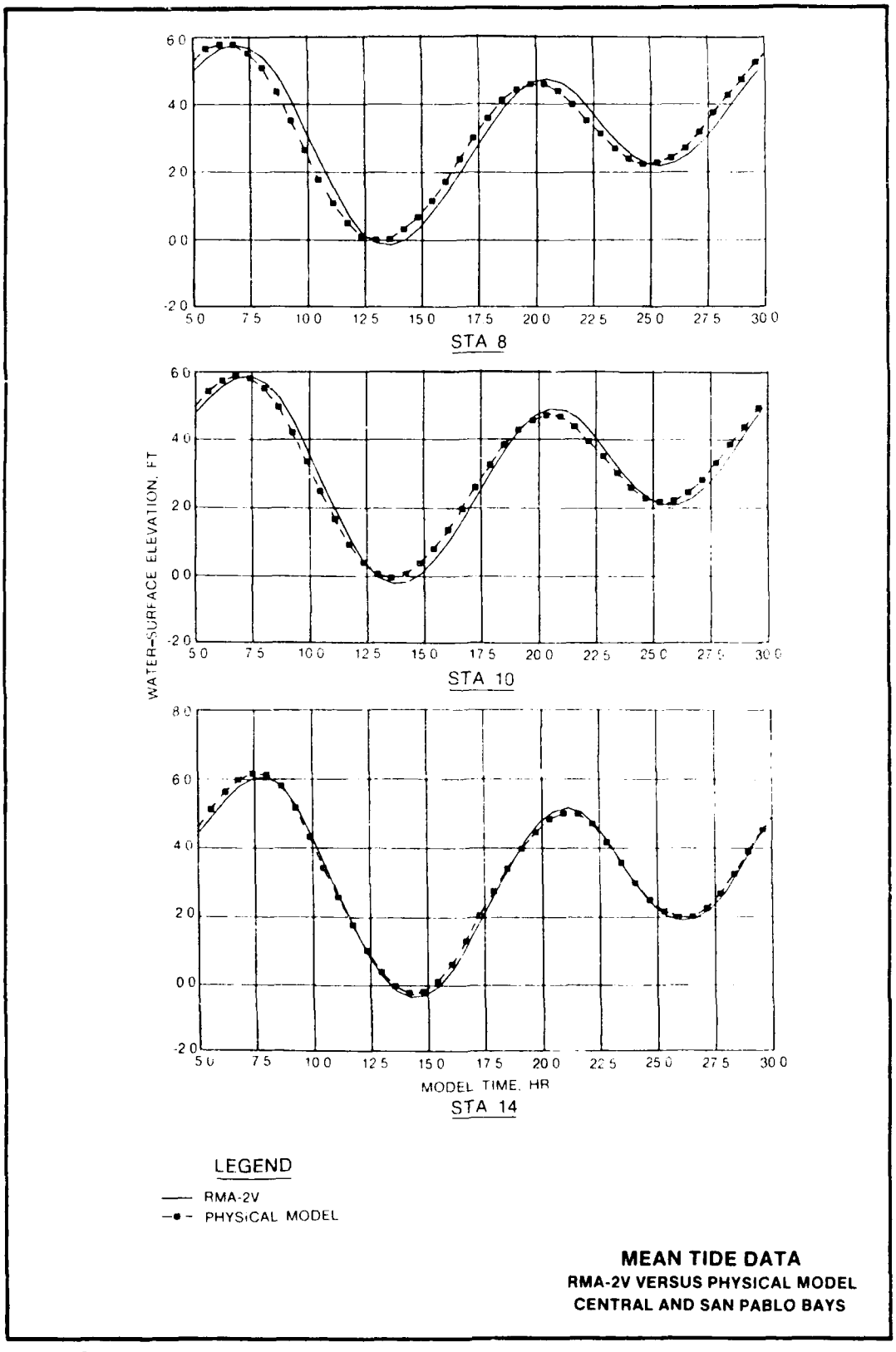

MEAN TIDE DATA
RMA-2V VERSUS PHYSICAL MODEL
CENTRAL AND SAN PABLO BAYS

PLATE 2

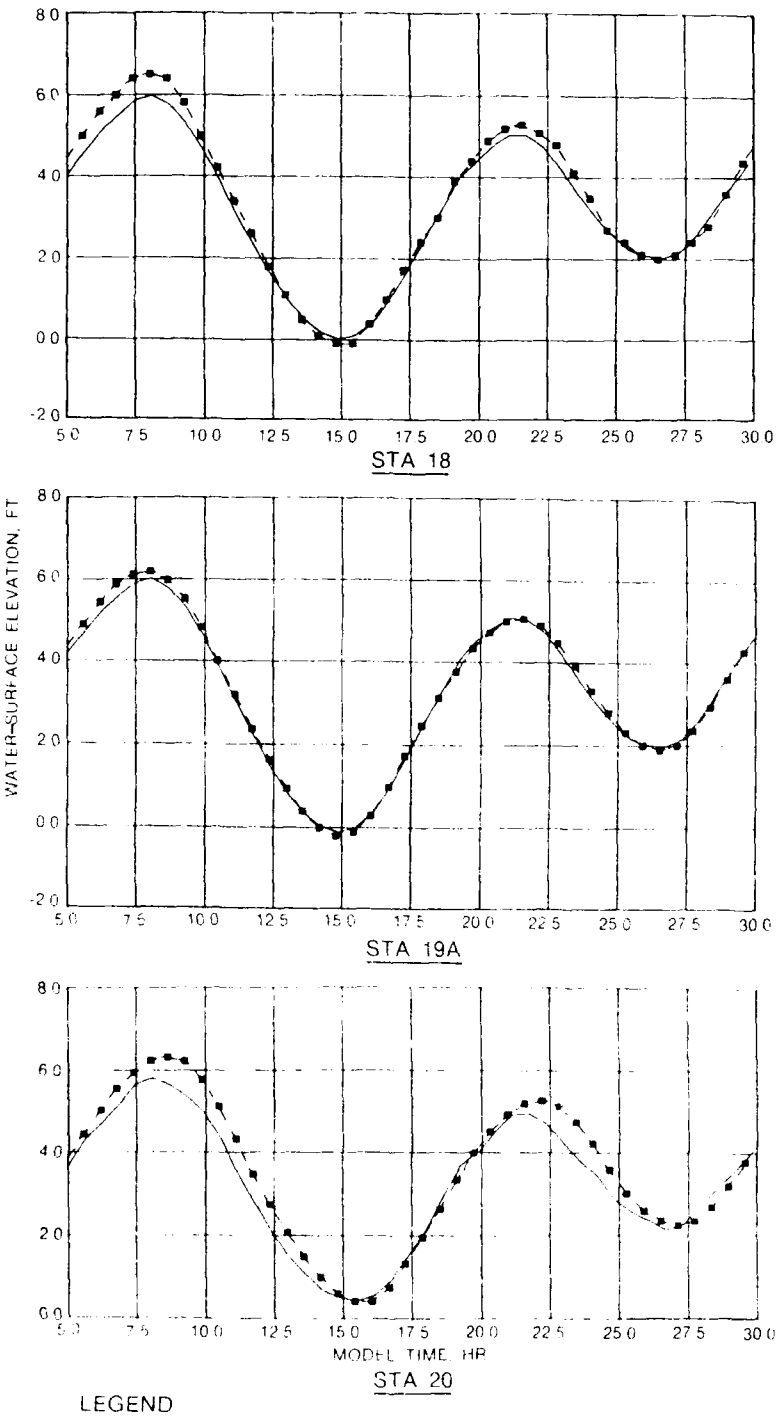

MEAN TIDE DATA
RMA-2V VERSUS PHYSICAL MODEL
MARE ISLAND AND CARQUINEZ STRAIT

PLATE 3

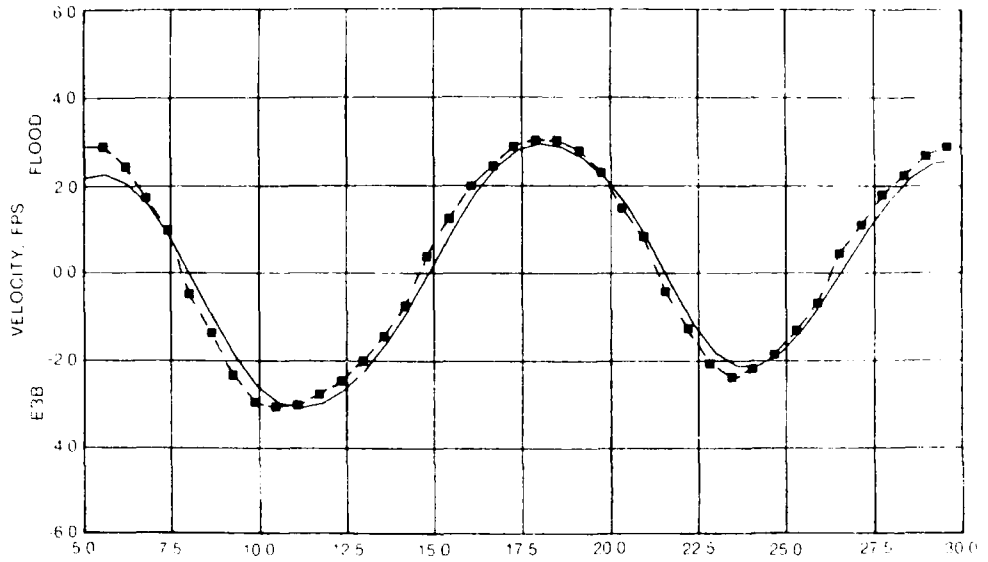

STA 2

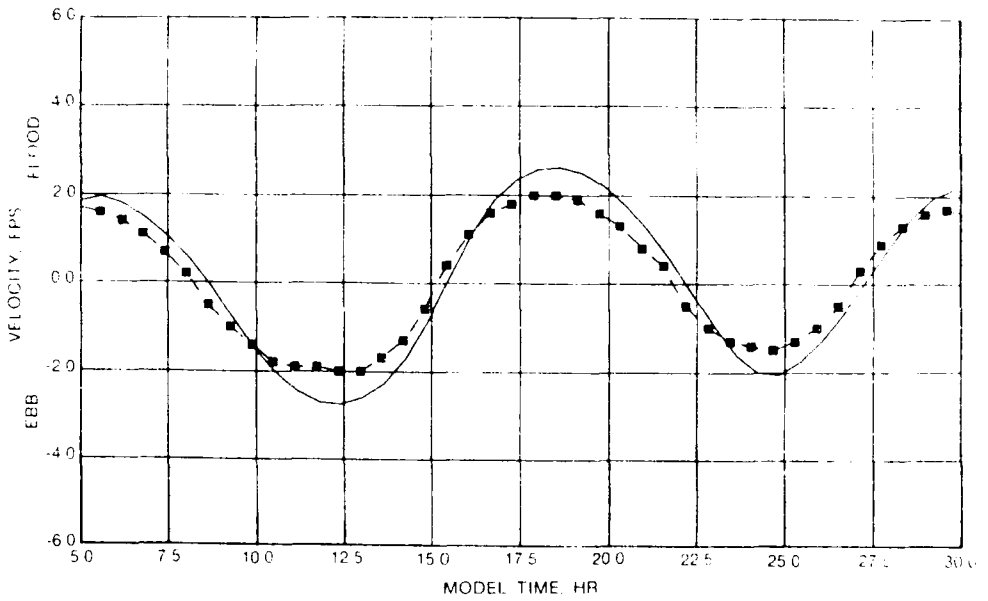

STA 2A

LEGEND

RMA-2V

PHYSICAL MODEL

MEAN TIDE VELOCITY DATA
RMA-2V VERSUS PHYSICAL MODEL
SOUTH BAY

PLATE 4

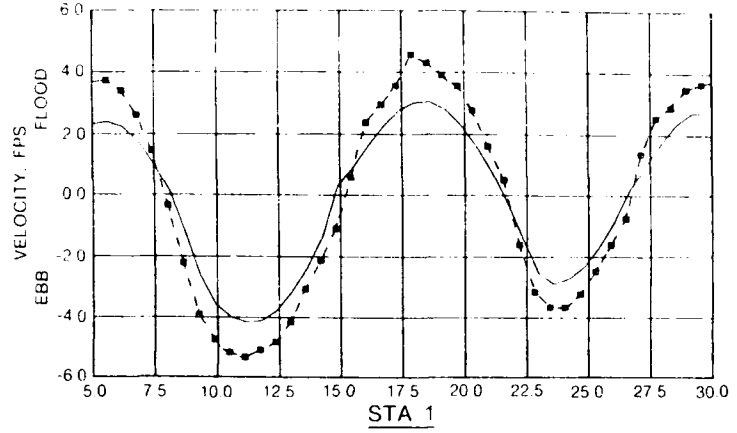

STA 1

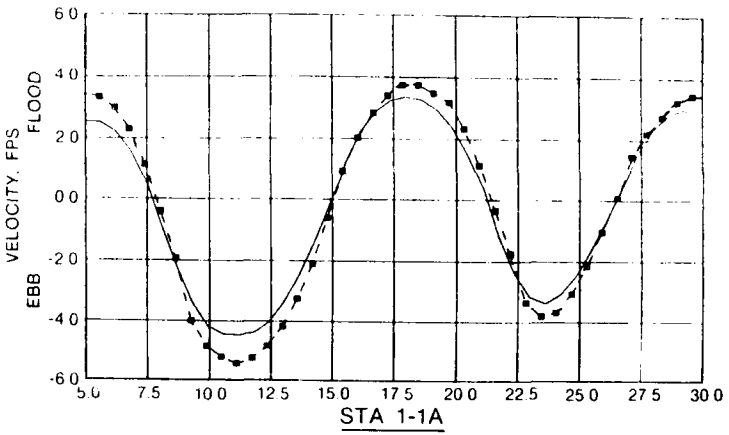

STA 1-1A

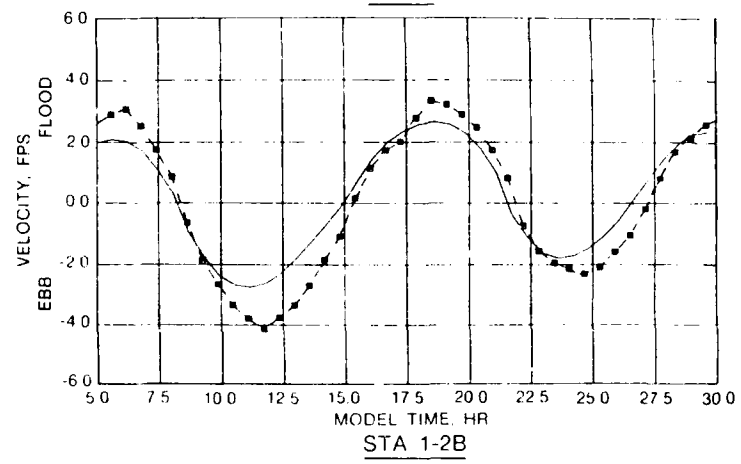

STA 1-2B

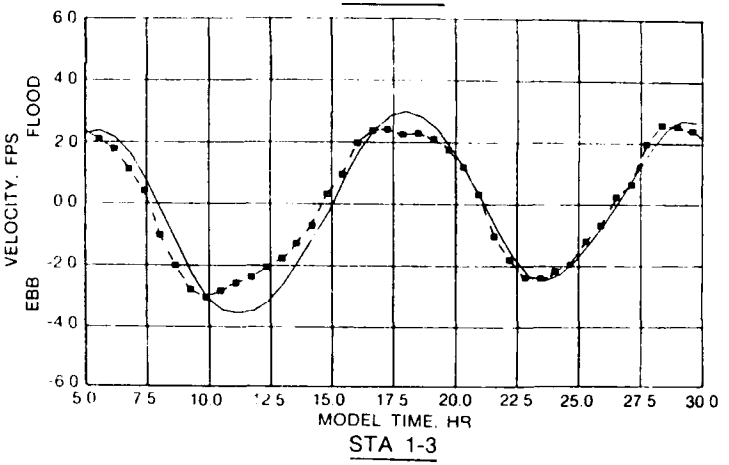

STA 1-3

LEGEND

- RMA-2V
- PHYSICAL MODEL

MEAN TIDE VELOCITY DATA
RMA-2V VERSUS PHYSICAL MODEL
CENTRAL BAY
STA 1, 1-1A, 1-2B, AND 1-3

PLATE 5

PLATE 6

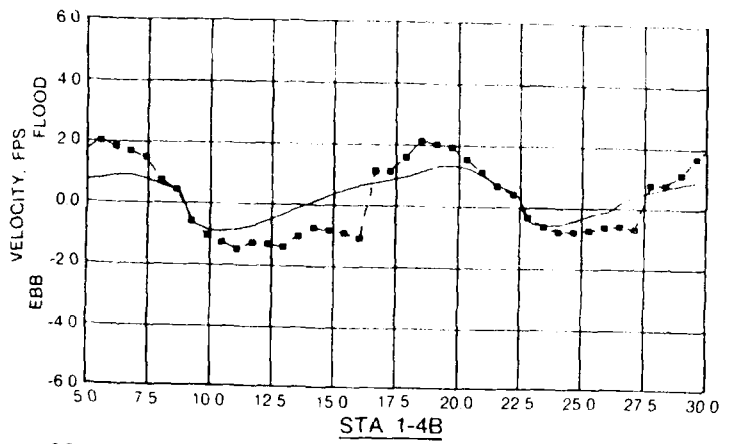

STA 1-4B

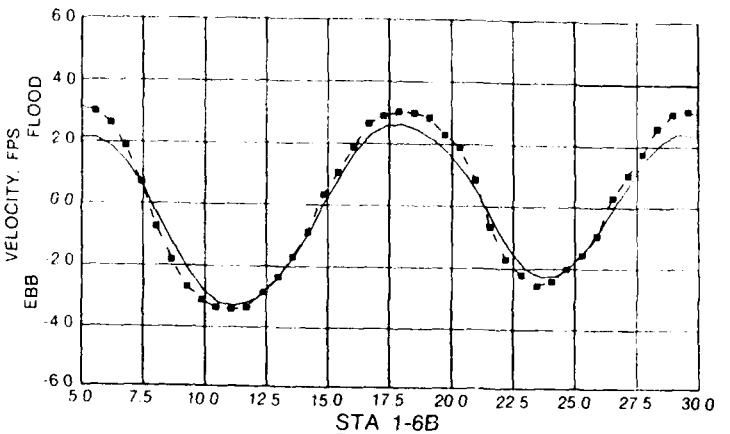

STA 1-6B

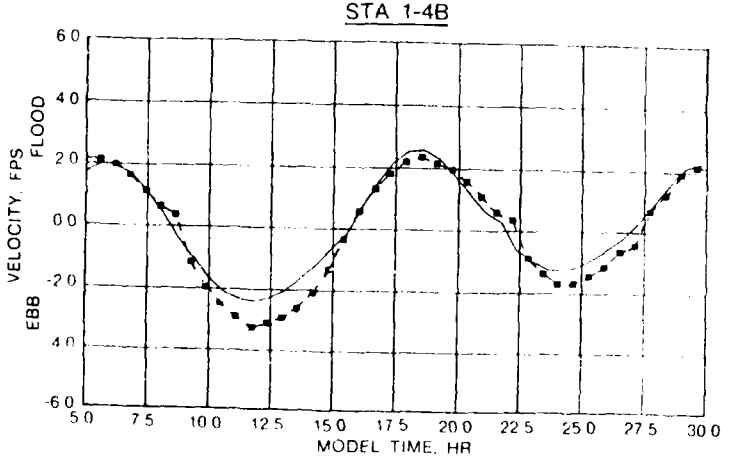

STA 3

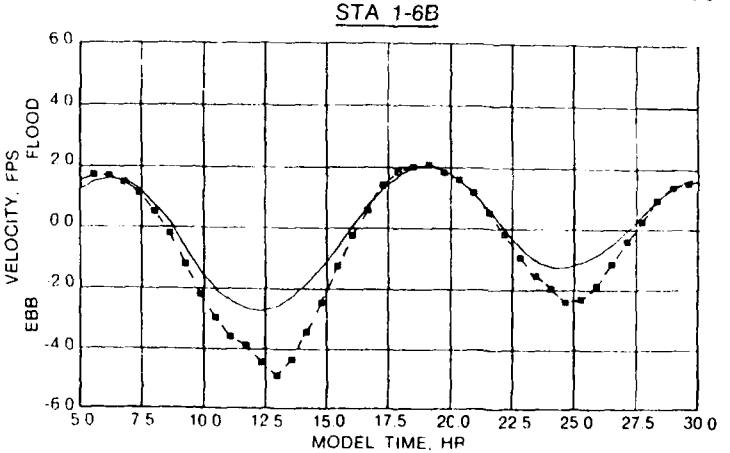

STA 3-2

LEGEND

— RMA-2V

—•— PHYSICAL MODEL

MEAN TIDE VELOCITY DATA

RMA-2V VERSUS PHYSICAL MODEL

CENTRAL BAY

STA 1-4B, 1-6B, 3, AND 3-2

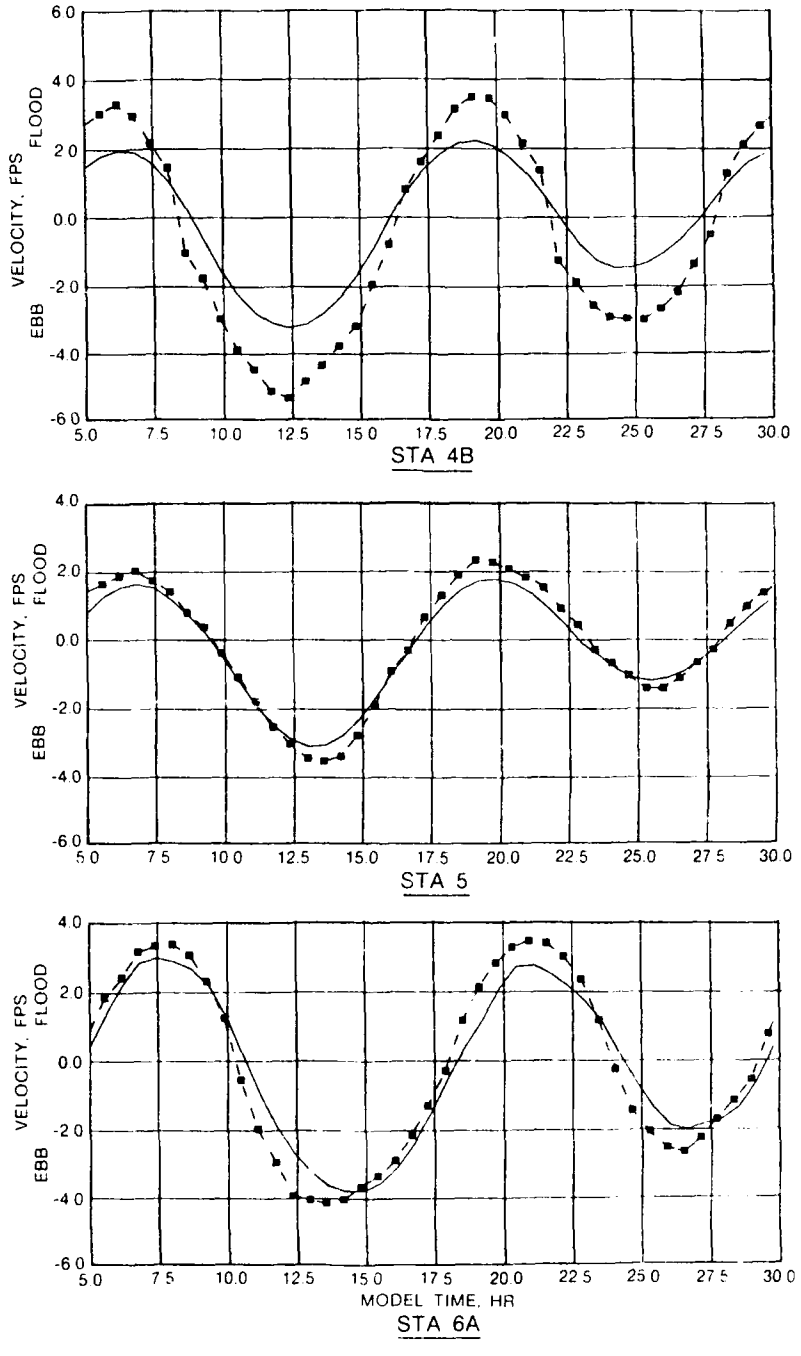

LEGEND

—— RMA-2V
—●— PHYSICAL MODEL

MEAN TIDE VELOCITY DATA
RMA-2V VERSUS PHYSICAL MODEL
SAN PABLO BAY AND CARQUINEZ STRAIT

PLATE 7

PLATE 8

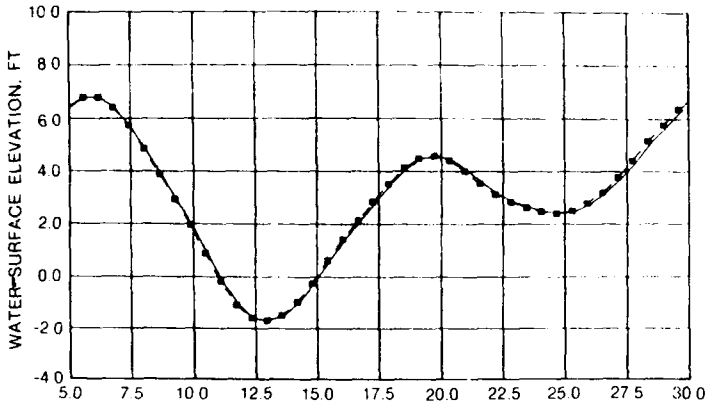

OCEAN STA 0

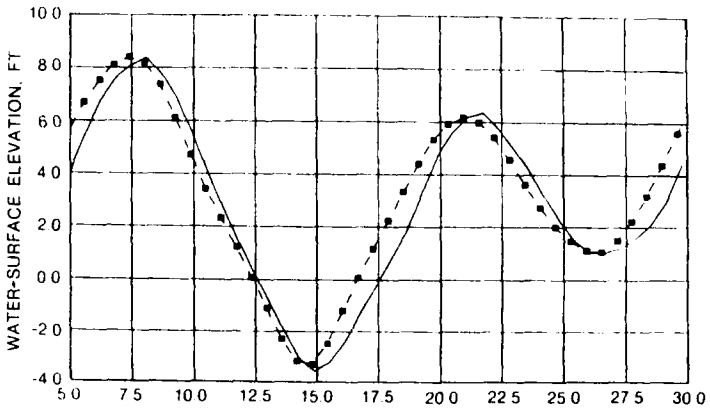

STA 2

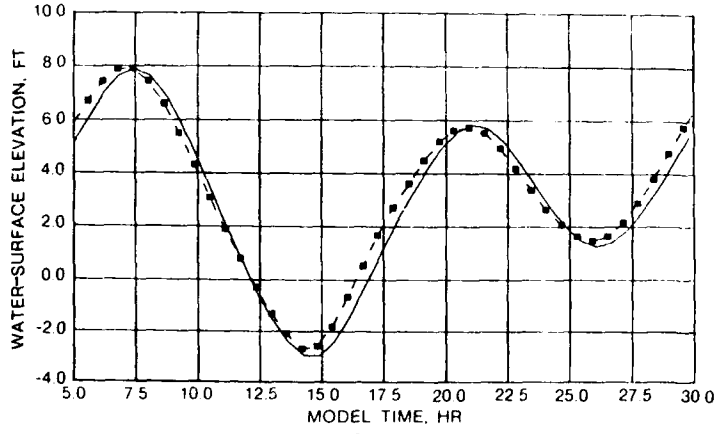

STA 3

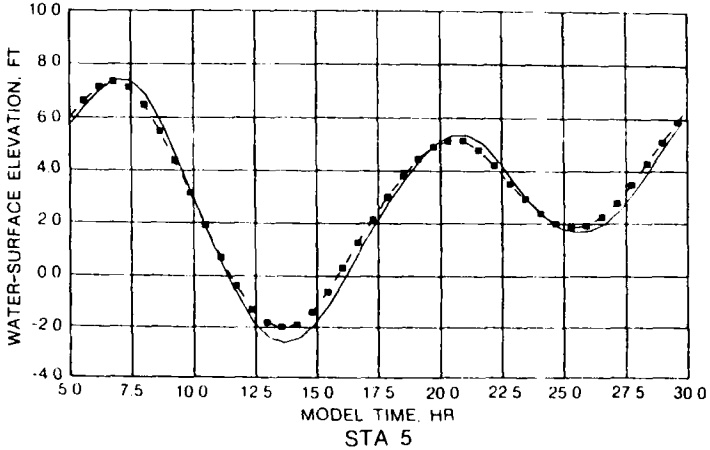

STA 5

LEGEND

RMA-2V

PHYSICAL MODEL

SPRING TIDE DATA

RMA-2V VERSUS PHYSICAL MODEL

OCEAN AND SOUTH BAY

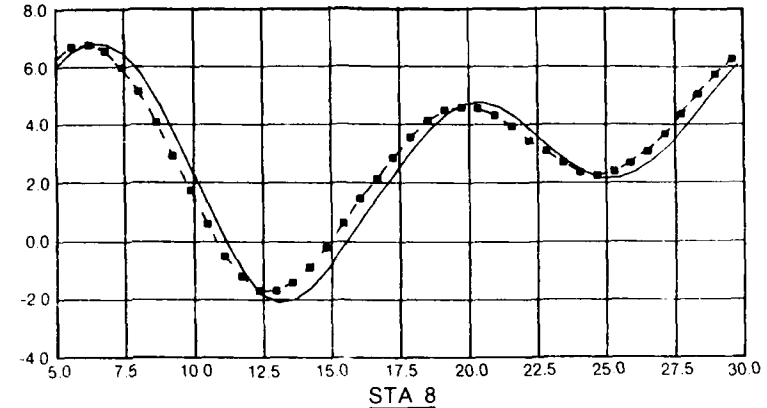

STA 8

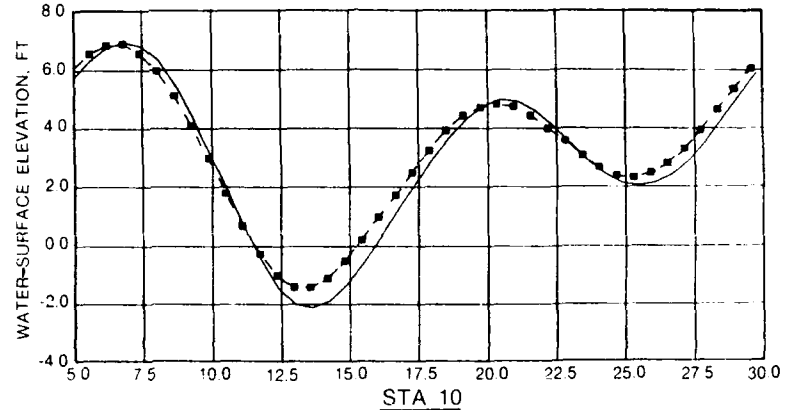

STA 10

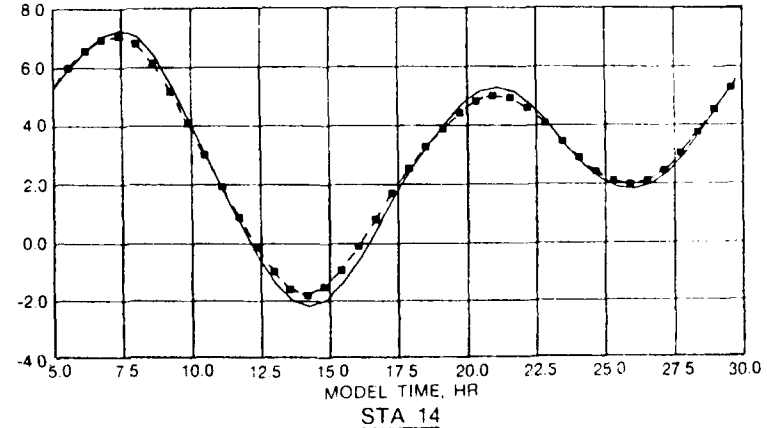

STA 14

LEGEND

—— RMA-2V

—●-- PHYSICAL MODEL

SPRING TIDE DATA

RMA-2V VERSUS PHYSICAL MODEL

CENTRAL AND SAN PABLO BAYS

PLATE 9

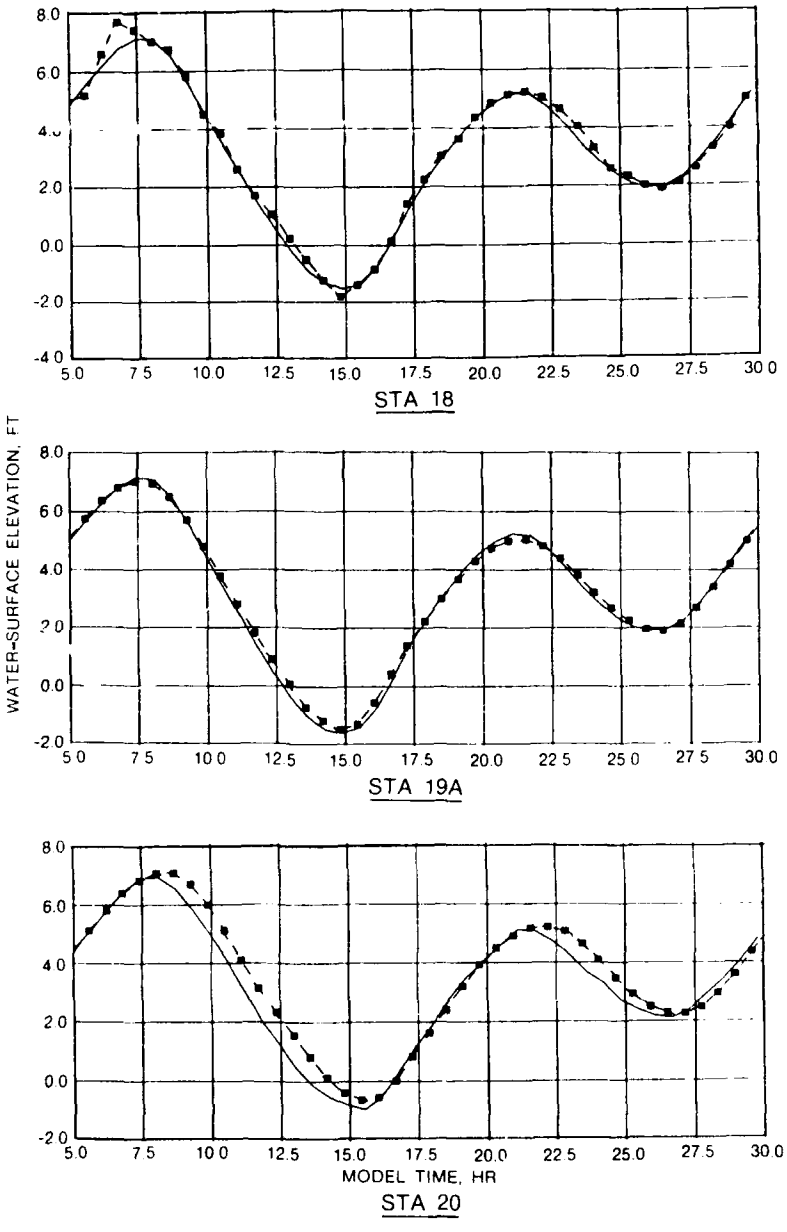

LEGEND

—— RMA-2V

—■— PHYSICAL MODEL

SPRING TIDE DATA

RMA-2V VERSUS PHYSICAL MODEL

MARE ISLAND AND CARQUINEZ STRAIT

PLATE 10

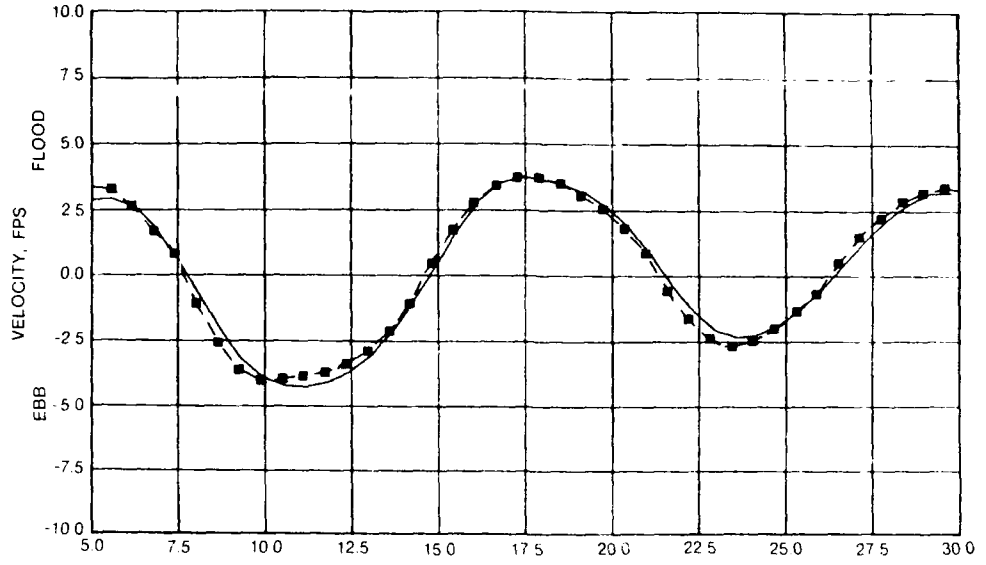

STA 2

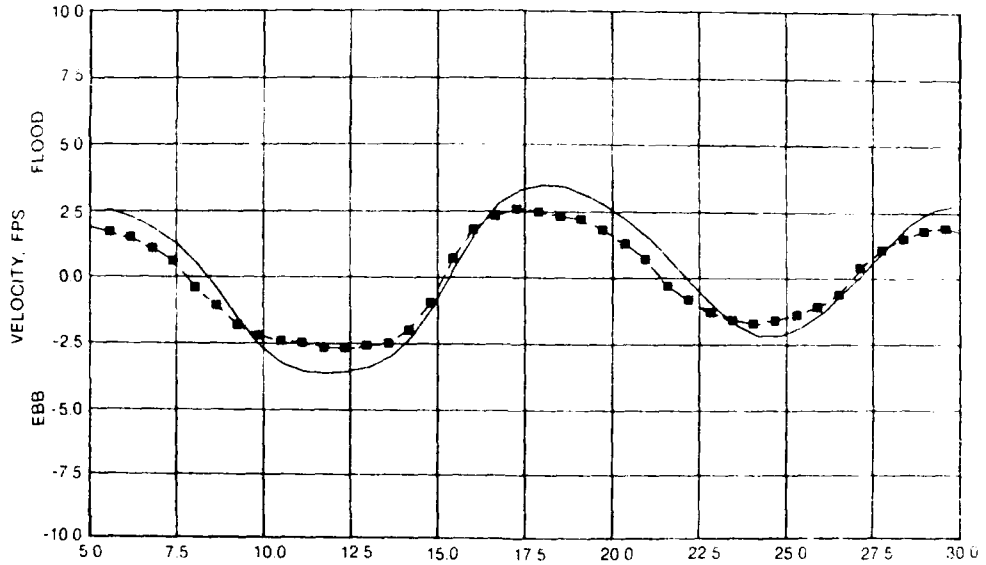

STA 2A

LEGEND

RMA-2V

PHYSICAL MODEL

SPRING TIDE VELOCITY DATA
RMA-2V VERSUS PHYSICAL MODEL
SOUTH BAY

PLATE 11

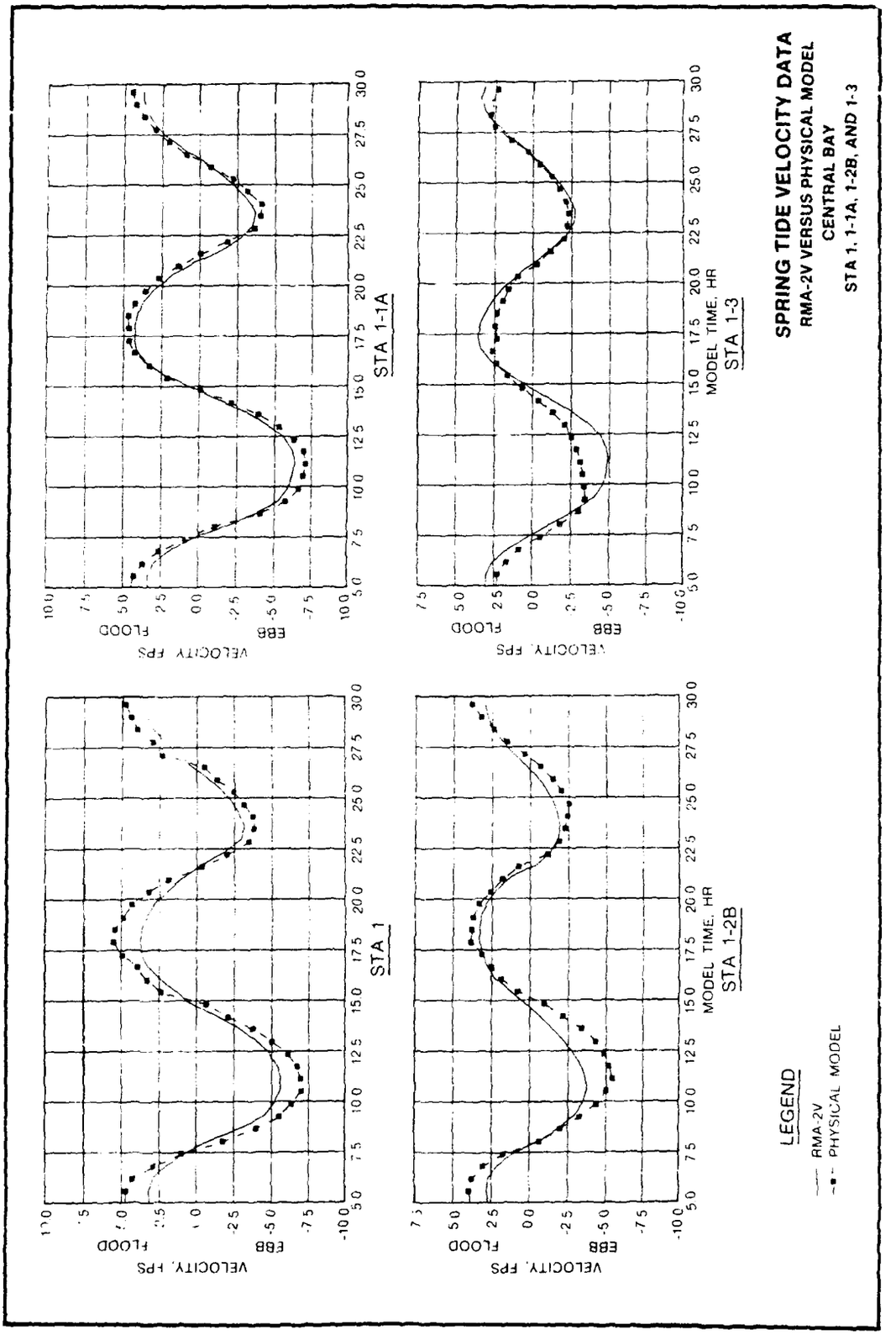
SPRING TIDE VELOCITY DATA
RMA-2V VERSUS PHYSICAL MODEL
CENTRAL BAY
STA 1, 1-1A, 1-2B, AND 1-3
STA 1-1A
STA 1-3
STA 1
STA 1-2B
VELOCITY, FPS
MODEL TIME, HR
EBB
FLOOD
LEGEND
RMA-2V
PHYSICAL MODEL

PLATE 12

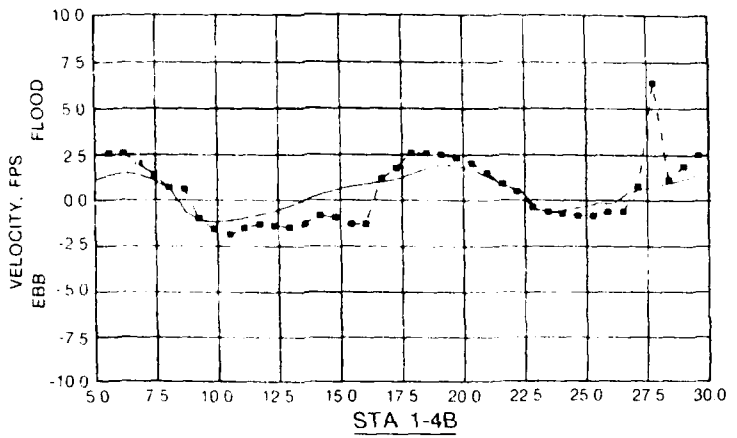

STA 1-4B

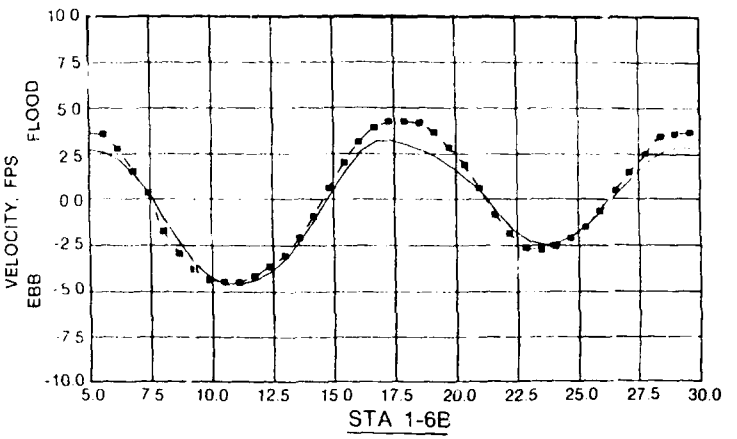

STA 1-6B

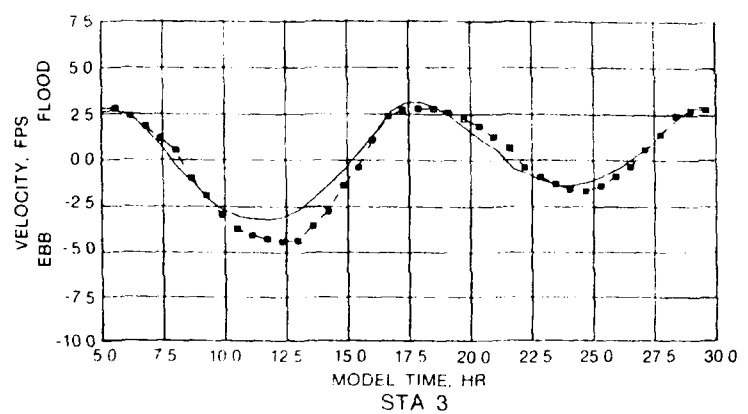

STA 3

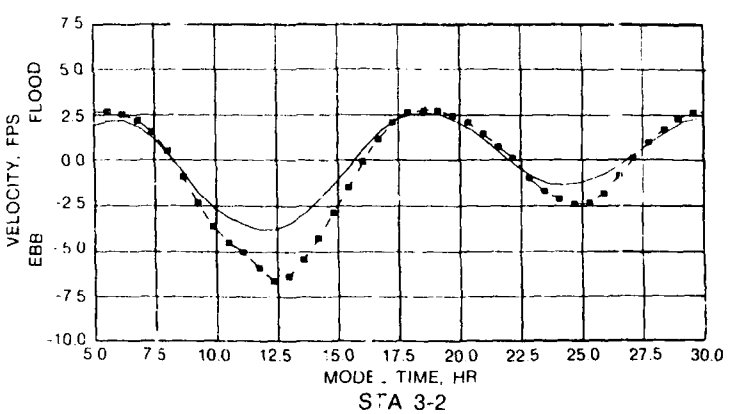

STA 3-2

LEGEND

—— RMA-2V

--■-- PHYSICAL MODEL

SPRING TIDE VELOCITY DATA

RMA-2V VERSUS PHYSICAL MODEL

CENTRAL BAY

STA 1-4B, 1-6B, 3, AND 3-2

PLATE 13

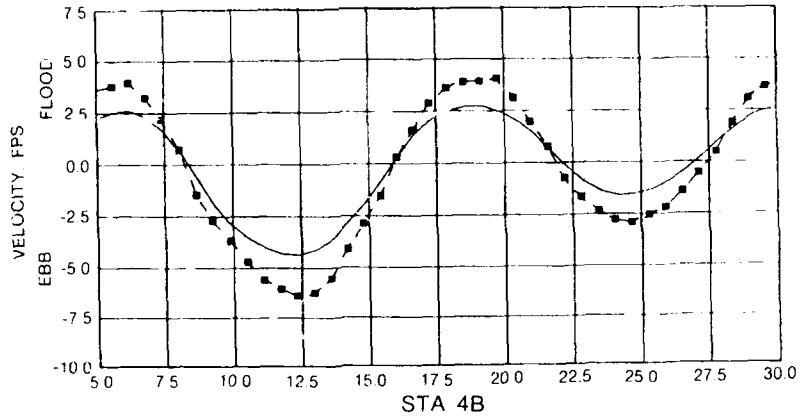

STA 4B

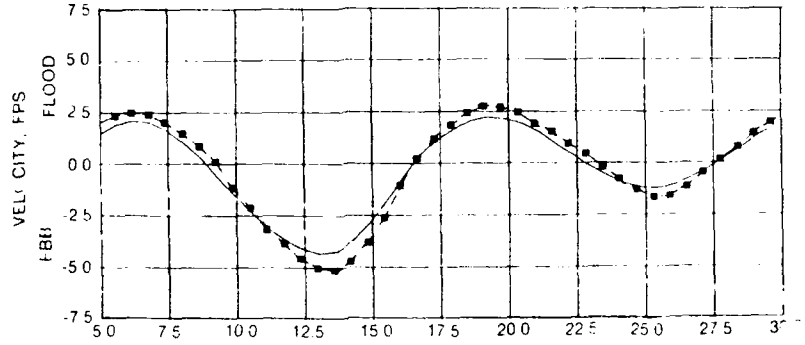

STA 5

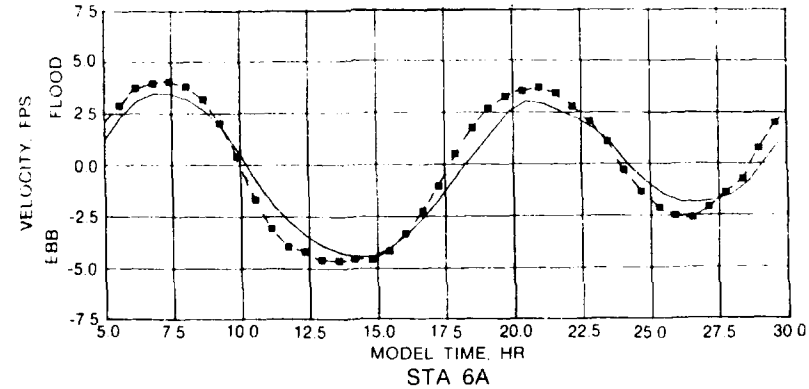

STA 6A

LEGEND

—— RMA-2V

·-●- PHYSICAL MODEL

SPRING TIDE VELOCITY DATA
RMA-2V VERSUS PHYSICAL MODEL
SAN PABLO BAY AND CARQUINEZ STRAIT

PLATE 14

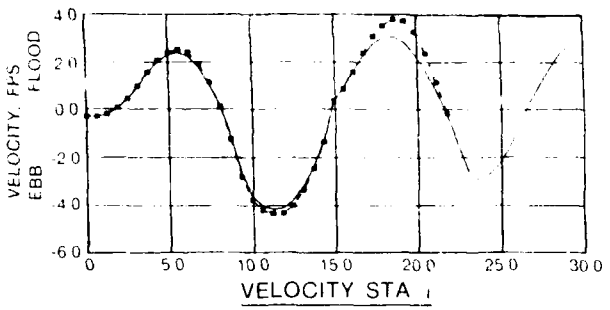

VELOCITY STA 1

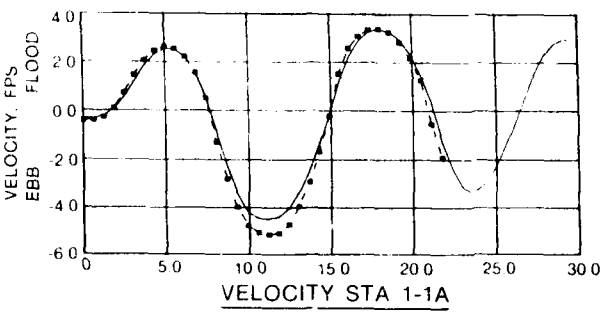

VELOCITY STA 1-1A

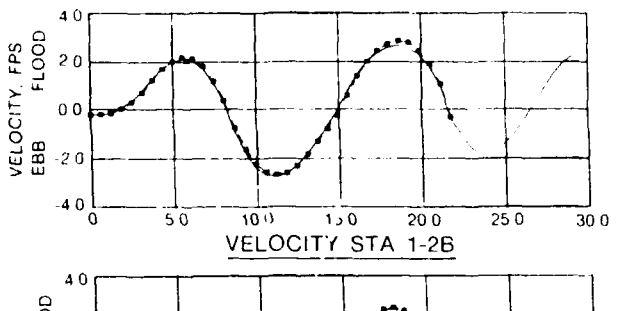

VELOCITY STA 1-2B

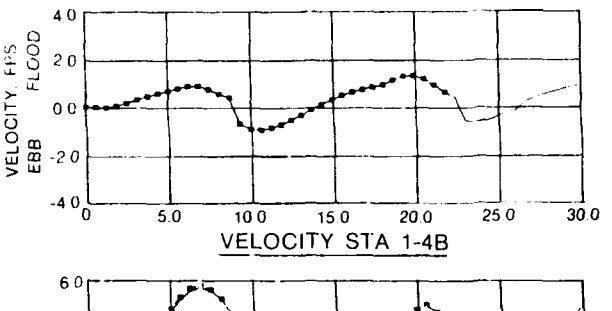

VELOCITY STA 1-4B

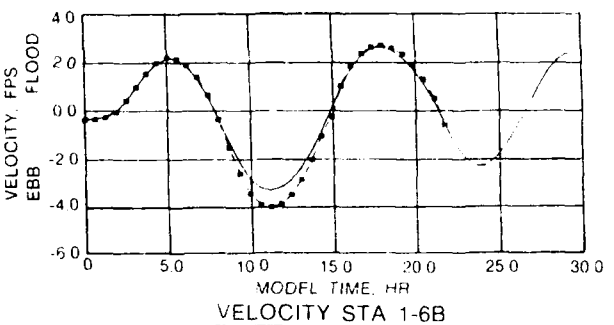

VELOCITY STA 1-6B

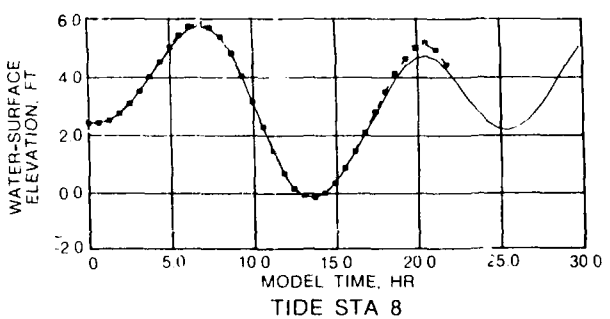

TIDE STA 8

LEGEND

— GLOBAL

-·- INSET MESH

MEAN TIDE DATA

GLOBAL VERSUS INSET MESH

CENTRAL BAY

PLATE 15

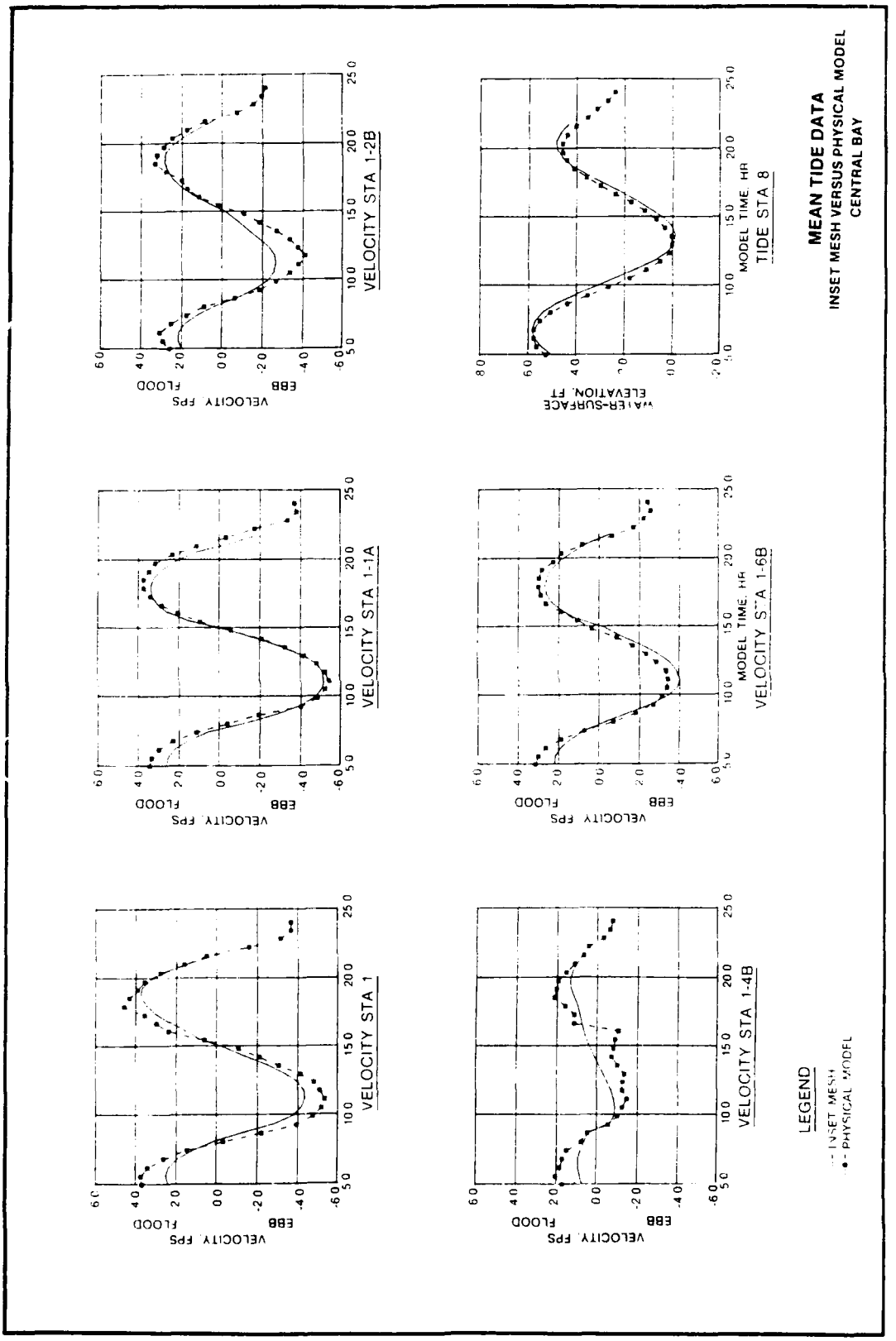
MEAN TIDE DATA
INSET MESH VERSUS PHYSICAL MODEL
CENTRAL BAY
TIDE STA 8
WATER-SURFACE ELEVATION, FT
MODEL TIME, HR
VELOCITY STA 1-2B
VELOCITY STA 1-6B
VELOCITY STA 1-1A
VELOCITY STA 1-4B
VELOCITY STA 1
VELOCITY, FPS
EBB
FLOOD
LEGEND
- INSET MESH
• PHYSICAL MODEL

PLATE 16

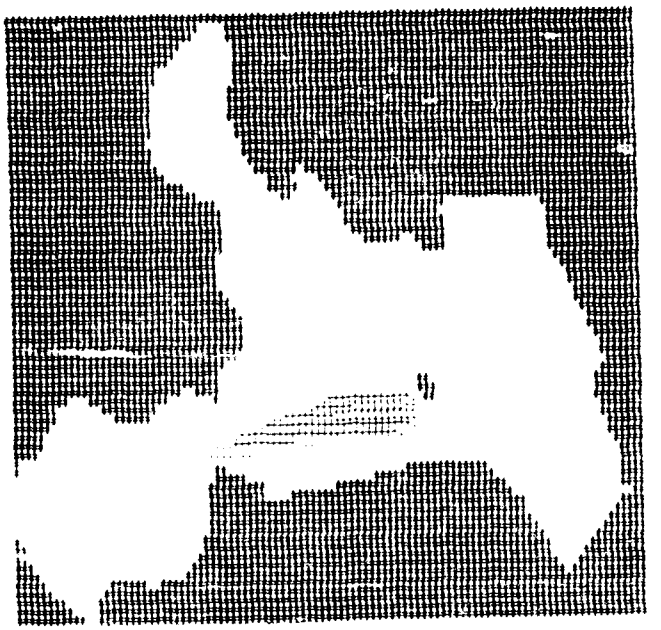

0.62 HR

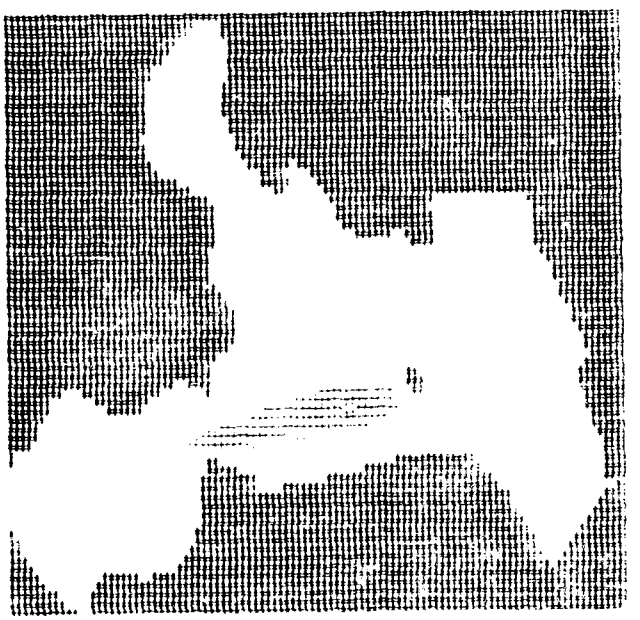

1.24 HR

SEDIMENT [illegible]
ABOVE BACKGROUND CONCENTRATION
0.0500 [illegible]
0.1001- [illegible]
1.0001-10.000 [illegible]

SUSPENDED SEDIMENT PATTERNS AT MAXIMUM EBB CURRENT VELOCITIES
0.62 AND 1.24 HR
AFTER DISPOSAL

PLATE 17

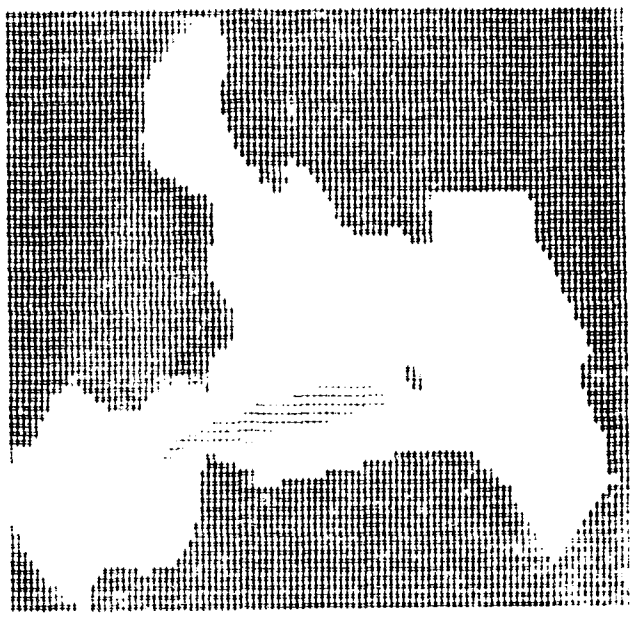

1.86 HR

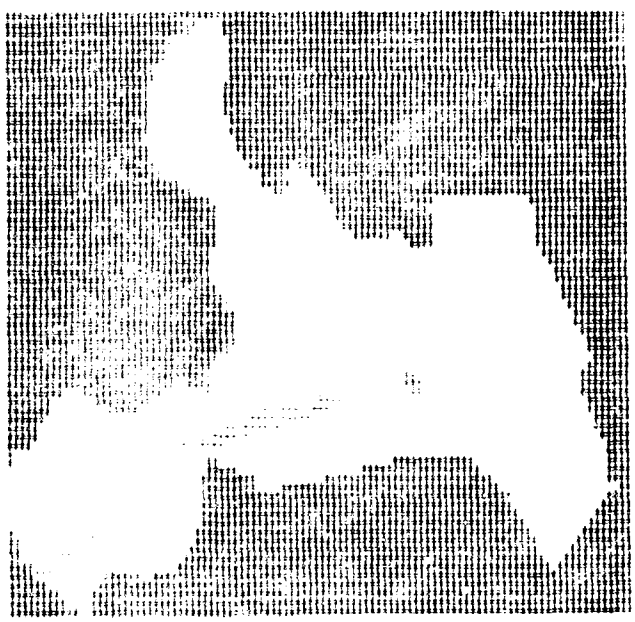

2.48 HR

SEDIMENT
ABOVE BACKGROUND
0.0500-
0.1001-
>.0001-10.00

SUSPENDED SEDIMENT PATTERNS AT MAXIMUM EBB CURRENT VELOCITIES
1.86 AND 2.48 HR
AFTER DISPOSAL

PLATE 18

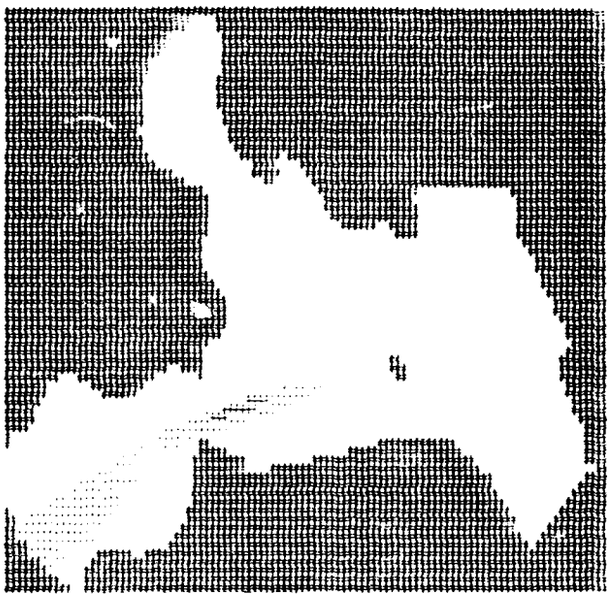

3.11 HR

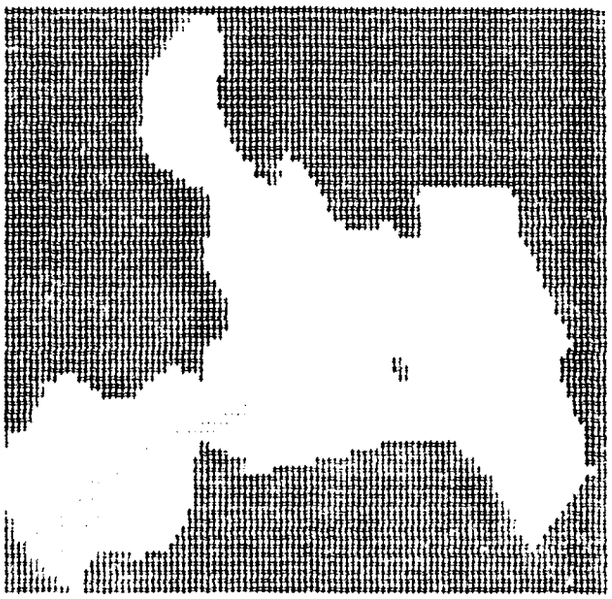

3.73 HR

SEDIMENT [illegible]
ABOVE BACKGROUND CONCENTRATION
0.0500- [illegible]
0.1001- [illegible]
0.0001 [illegible]

SUSPENDED SEDIMENT PATTERNS AT MAXIMUM EBB CURRENT VELOCITIES
3.11 AND 3.73 HR
AFTER DISPOSAL

PLATE 19

APPENDIX A: THE TABS-2 SYSTEM

1. TABS-2 is a collection of generalized computer programs and utility codes integrated into a numerical modeling system for studying two-dimensional hydrodynamics, sedimentation, and transport problems in rivers, reservoirs, bays, and estuaries. A schematic representation of the system is shown in Figure A1. It can be used either as a stand-alone solution technique or as a step in the hybrid modeling approach. The basic concept is to calculate water-surface elevations, current patterns, sediment erosion, transport and deposition, the resulting bed surface elevations, and the feedback to hydraulics. Existing and proposed geometry can be analyzed to determine the impact on sedimentation of project designs and to determine the impact of project designs on salinity and on the stream system. The system is described in detail by Thomas and McAnally (1985).

2. The three basic components of the system are as follows:

   a. "A Two-Dimensional Model for Free Surface Flows," RMA-2V.

   b. "Sediment Transport in Unsteady 2-Dimensional Flows, Horizontal Plane," STUDH.

   c. "Two-Dimensional Finite Element Program for Water Quality," RMA-4.

3. RMA-2V is a finite element solution of the Reynolds form of the Navier-Stokes equations for turbulent flows. Friction is calculated with Manning's equation and eddy viscosity coefficients are used to define the turbulent losses. A velocity form of the basic equation is used with side boundaries treated as either slip or static. The model automatically recognizes dry elements and corrects the mesh accordingly. Boundary conditions may be water-surface elevations, velocities, or discharges and may occur inside the mesh as well as along the edges.

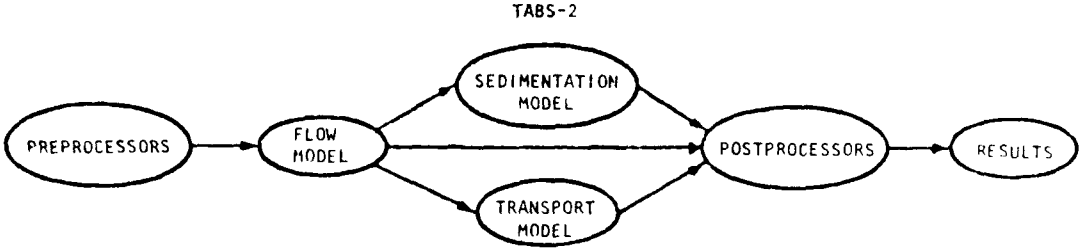

Figure A1. TABS-2 schematic

4. The sedimentation model, STUDH, solves the convection-diffusion equation with bed source terms. These terms are structured for either sand or cohesive sediments. The Ackers-White (1973) procedure is used to calculate a sediment transport potential for the sands from which the actual transport is calculated based on availability. Clay erosion is based on work by Partheniades (1962) and Ariathurai and the deposition of clay utilizes Krone's equations (Ariathurai, MacArthur, and Krone 1977). Deposited material forms layers, as shown in Figure A2, and bookkeeping allows up to 10 layers at each node for maintaining separate material types, deposit thickness, and age. The code uses the same mesh as RMA-2V.

5. Salinity calculations, RMA-4, are made with a form of the convective-diffusion equation which has general source-sink terms. Up to seven conservative substances or substances requiring a decay term can be routed. The code uses the same mesh as RMA-2V.

6. Each of these generalized computer codes can be used as a stand-alone program, but to facilitate the preparation of input data and to aid in analyzing results, a family of utility programs was developed for the following purposes:

a. Digitizing
b. Mesh generation
c. Spatial data management
d. Graphical output
e. Output analysis
f. File management
g. Interfaces
h. Job control language

Finite Element Modeling

7. The TABS-2 numerical models used in this effort employ the finite element method to solve the governing equations. To help those who are unfamiliar with the method to better understand this report, a brief description of the method is given here.

8. The finite element method approximates a solution to equations by dividing the area of interest into smaller subareas, which are called elements. The dependent variables (e.g., water-surface elevations and sediment

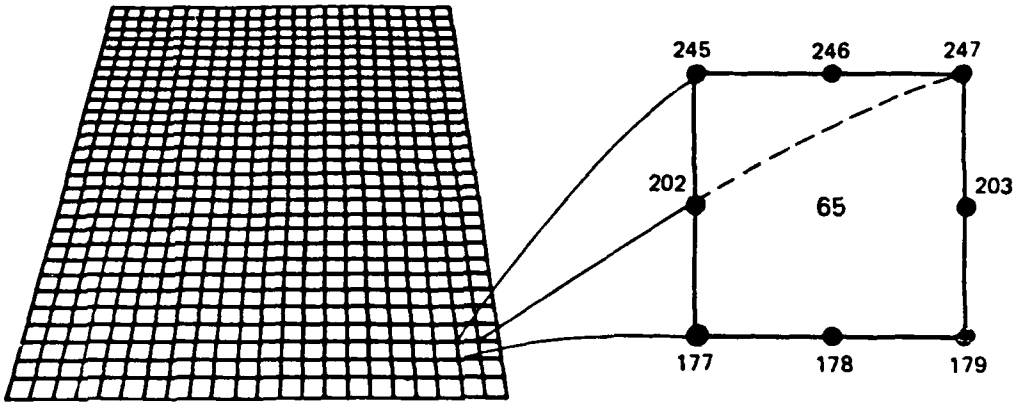

a. Eight nodes define each element

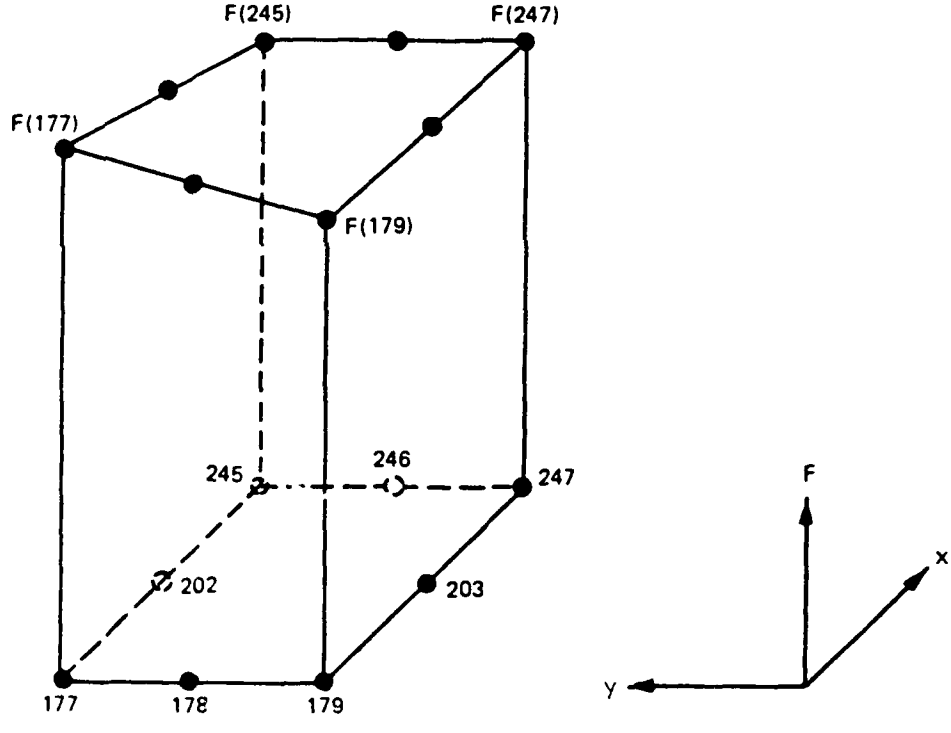

b. Linear interpolation function

Figure A2. Two-dimensional finite element mesh

concentrations) are approximated over each element by continuous functions which interpolate in terms of unknown point (node) values of the variables. An error, defined as the deviation of the approximation solution from the correct solution, is minimized. Then, when boundary conditions are imposed, a set of solvable simultaneous equations is created. The solution is continuous over the area of interest.

9. In one-dimensional problems, elements are line segments. In two-dimensional problems, the elements are polygons, usually either triangles or quadrilaterals. Nodes are located on the edges of elements and occasionally inside the elements. The interpolating functions may be linear or higher order polynomials. Figure A2 illustrates a quadrilateral element with eight nodes and a linear solution surface where F is the interpolating function.

10. Most water resource applications of the finite element method use the Galerkin method of weighted residuals to minimize error. In this method the residual, the total error between the approximate and correct solutions, is weighted by a function that is identical with the interpolating function and then minimized. Minimization results in a set of simultaneous equations in terms of nodal values of the dependent variable (e.g. water-surface elevations or sediment concentration). The time portion of time-dependent problems can be solved by the finite element method, but it is generally more efficient to express derivatives with respect to time in finite difference form.

The Hydrodynamic Model, RMA-2V

Applications

11. This program is designed for far-field problems in which vertical accelerations are negligible and the velocity vectors at a node generally point in the same directions over the entire depth of the water column at any instant of time. It expects a homogeneous fluid with a free surface. Both steady and unsteady state problems can be analyzed. A surface wind stress can be imposed.

12. The program has been applied to calculate flow distribution around islands; flow at bridges having one or more relief openings, in contracting and expanding reaches, into and out of off-channel hydropower plants, at river junctions, and into and out of pumping plant channels; and general flow patterns in rivers, reservoirs, and estuaries.

Limitations

13. This program is not designed for near-field problems where flow-structure interactions (such as vortices, vibrations, or vertical accelerations) are of interest. Areas of vertically stratified flow are beyond this program's capability unless it is used in a hybrid modeling approach. It is two-dimensional in the horizontal plane, and zones where the bottom current is in a different direction from the surface current must be analyzed with considerable subjective judgement regarding long-term energy considerations. It is a free-surface calculation for subcritical flow problems.

Governing equations

14. The generalized computer program RMA-2V solves the depth-integrated equations of fluid mass and momentum conservation in two horizontal directions. The form of the solved equations is

$$h\frac{\partial u}{\partial t} + hu\frac{\partial u}{\partial x} + hv\frac{\partial u}{\partial y} - \frac{h}{\rho}\left(\epsilon_{xx}\frac{\partial^2 u}{\partial x^2} + \epsilon_{xy}\frac{\partial^2 u}{\partial y^2}\right) + gh\left(\frac{\partial a}{\partial x} + \frac{\partial h}{\partial x}\right)$$

$$+ \frac{gun^2}{\left(1.486h^{1/6}\right)^2}\left(u^2 + v^2\right)^{1/2} - \zeta V_a^2 \cos\psi - 2h\omega v \sin\phi = 0 \qquad \text{(A1)}$$

$$h\frac{\partial v}{\partial t} + hu\frac{\partial v}{\partial x} + hv\frac{\partial v}{\partial y} - \frac{h}{\rho}\left(\epsilon_{yx}\frac{\partial^2 v}{\partial x^2} + \epsilon_{yy}\frac{\partial^2 v}{\partial y^2}\right) + gh\left(\frac{\partial a}{\partial y} + \frac{\partial h}{\partial y}\right)$$

$$+ \frac{gvn^2}{\left(1.486h^{1/6}\right)^2}\left(u^2 + v^2\right)^{1/2} - \zeta V_a^2 \sin\psi + 2\omega hu \sin\phi = 0 \qquad \text{(A2)}$$

$$\frac{\partial h}{\partial t} + h\left(\frac{\partial u}{\partial x} + \frac{\partial v}{\partial y}\right) + u\frac{\partial h}{\partial x} + v\frac{\partial h}{\partial y} = 0 \qquad \text{(A3)}$$

where

h = depth

u,v = velocities in the Cartesian directions

x,y,t = Cartesian coordinates and time

ρ = density

ε = eddy viscosity coefficient, for xx = normal direction on x-axis surface; yy = normal direction on y-axis surface; xy and yx = shear direction on each surface

g = acceleration due to gravity

a = elevation of bottom

n = Manning's n value

1.486 = conversion from SI (metric) to non-SI units

ζ = empirical wind shear coefficient

V_a = wind speed

ψ = wind direction

ω = rate of earth's angular rotation

ϕ = local latitude

15. Equations A1, A2, and A3 are solved by the finite element method using Galerkin weighted residuals. The elements may be either quadrilaterals or triangles and may have curved (parabolic) sides. The shape functions are quadratic for flow and linear for depth. Integration in space is performed by Gaussian integration. Derivatives in time are replaced by a nonlinear finite difference approximation. Variables are assumed to vary over each time interval in the form

$$f(t) = f(0) + at + bt^c \qquad t_0 \leq t < t \tag{A4}$$

which is differentiated with respect to time, and cast in finite difference form. Letters a, b, and c are constants. It has been found by experiment that the best value for c is 1.5 (Norton and King 1977).

16. The solution is fully implicit and the set of simultaneous equations is solved by Newton-Raphson iteration. The computer code executes the solution by means of a front-type solver that assembles a portion of the matrix and solves it before assembling the next portion of the matrix. The front solver's efficiency is largely independent of bandwidth and thus does not require as much care in formation of the computational mesh as do traditional solvers.

17. The code RMA-2V is based on the earlier version RMA-2 (Norton and King 1977) but differs from it in several ways. It is formulated in terms of velocity (v) instead of unit discharge (vh), which improves some aspects of the code's behavior; it permits drying and wetting of areas within the grid;

and it permits specification of turbulent exchange coefficients in directions other than along the x- and z-axes. For a more complete description, see Appendix F of Thomas and McAnally (1985).

The Sediment Transport Model, STUDH

Applications

18. STUDH can be applied to clay and/or sand bed sediments where flow velocities can be considered two-dimensional (i.e., the speed and direction can be satisfactorily represented as a depth-averaged velocity). It is useful for both deposition and erosion studies and, to a limited extent, for stream width studies. The program treats two categories of sediment: noncohesive, which is referred to as sand here, and cohesive, which is referred to as clay.

Limitations

19. Both clay and sand may be analyzed, but the model considers a single, effective grain size for each and treats each separately. Fall velocity must be prescribed along with the water-surface elevations, x-velocity, y-velocity, diffusion coefficients, bed density, critical shear stresses for erosion, erosion rate constants, and critical shear stress for deposition.

20. Many applications cannot use long simulation periods because of their computation cost. Study areas should be made as small as possible to avoid an excessive number of elements when dynamic runs are contemplated yet must be large enough to permit proper posing of boundary conditions. The same computation time interval must be satisfactory for both the transverse and longitudinal flow directions.

21. The program does not compute water-surface elevations or velocities; therefore these data must be provided. For complicated geometries, the numerical model for hydrodynamic computations, RMA-2V, is used.

Governing equations

22. The generalized computer program STUDH solves the depth-integrated convection-dispersion equation in two horizontal dimensions for a single sediment constituent. For a more complete description, see Appendix G of Thomas and McAnally (1985). The form of the solved equation is

$$\frac{\partial C}{\partial t} + u\frac{\partial C}{\partial x} + v\frac{\partial C}{\partial y} = \frac{\partial}{\partial x}\left(D_x\frac{\partial C}{\partial x}\right) + \frac{\partial}{\partial y}\left(D_y\frac{\partial C}{\partial y}\right) + \alpha_1 C + \alpha_2 = 0 \qquad (A5)$$

where

C = concentration of sediment

u = depth-integrated velocity in x-direction

v = depth-integrated velocity in y-direction

D_x = dispersion coefficient in x-direction

D_y = dispersion coefficient in y-direction

α_1 = coefficient of concentration-dependent source/sink term

α_2 = coefficient of source/sink term

23. The source/sink terms in Equation A5 are computed in routines that treat the interaction of the flow and the bed. Separate sections of the code handle computations for clay bed and sand bed problems.

Sand transport

24. The source/sink terms are evaluated by first computing a potential sand transport capacity for the specified flow conditions, comparing that capacity with the amount of sand actually being transported, and then eroding from or depositing to the bed at a rate that would approach the equilibrium value after sufficient elapsed time.

25. The potential sand transport capacity in the model is computed by the method of Ackers and White (1973), which uses a transport power (work rate) approach. It has been shown to provide superior results for transport under steady-flow conditions (White, Milli, and Crabbe 1975) and for combined waves and currents (Swart 1976). Flume tests at the US Army Engineer Waterways Experiment Station have shown that the concept is valid for transport by estuarine currents.

26. The total load transport function of Ackers and White is based upon a dimensionless grain size

$$D_{gr} = D\left[\frac{g(s - 1)}{\nu^2}\right]^{1/3} \tag{A6}$$

where

D = sediment particle diameter

s = specific gravity of the sediment

ν = kinematic viscosity of the fluid

and a sediment mobility parameter

$$F_{gr} = \left[\frac{\tau^{n'}\tau'^{(1-n')}}{\rho g D(s-1)}\right]^{1/2} \tag{A7}$$

where

τ = total boundary shear stress

n' = a coefficient expressing the relative importance of bed-load and suspended-load transport, given in Equation A9

τ' = boundary surface shear stress

The surface shear stress is that part of the total shear stress which is due to the rough surface of the bed only, i.e., not including that part due to bed forms and geometry. It therefore corresponds to that shear stress that the flow would exert on a plane bed.

27. The total sediment transport is expressed as an effective concentration

$$G_p = C\left(\frac{F_{gr}}{A} - 1\right)^m \frac{sD}{h}\left(\frac{\rho}{\tau} U\right)^{n'} \tag{A8}$$

where U is the average flow speed, and for $1 < D_{gr} \leq 60$

$$n' = 1.00 - 0.56 \log D_{gr} \tag{A9}$$

$$A = \frac{0.23}{\sqrt{D_{gr}}} + 0.14 \tag{A10}$$

$$\log C = 2.86 \log D_{gr} - (\log D_{gr})^2 - 3.53 \tag{A11}$$

$$m = \frac{9.66}{D_{gr}} + 1.34 \tag{A12}$$

For $D_{gr} < 60$

$$n' = 0.00 \tag{A13}$$

$$A = 0.17 \tag{A14}$$

$$C = 0.025 \tag{A15}$$

$$m = 1.5 \tag{A16}$$

28. Equations A6-A16 result in a potential sediment concentration G_p. This value is the depth-averaged concentration of sediment that will occur if an equilibrium transport rate is reached with a nonlimited supply of sediment. The rate of sediment deposition (or erosion) is then computed as

$$R = \frac{G_p - C}{t_c} \tag{A17}$$

where

C = present sediment concentration

t_c = time constant

For deposition, the time constant is

$$t_c = \text{larger of} \begin{cases} \Delta t \\ \text{or} \\ \dfrac{C_d h}{V_s} \end{cases} \tag{A18}$$

and for erosion it is

$$t_c = \text{larger of} \begin{cases} \Delta t \\ \text{or} \\ \dfrac{C_e h}{U} \end{cases} \tag{A19}$$

where

Δt = computational time-step

C_d = response time coefficient for deposition

V_s = sediment settling velocity

C_e = response time coefficient for erosion

The sand bed has a specified initial thickness which limits the amount of erosion to that thickness.

Cohesive sediments transport

29. Cohesive sediments (usually clays and some silts) are considered to be depositional if the bed shear stress exerted by the flow is less than a critical value τ_d. When that value occurs, the deposition rate is given by Krone's (1962) equation

$$S = \begin{cases} -\frac{2V_s}{h} C \left(1 - \frac{\tau}{\tau_d}\right) & \text{for } C < C_c \quad \text{(A20)} \\ -\frac{2V_s}{hC_c^{4/3}} C^{5/3} \left(1 - \frac{\tau}{\tau_d}\right) & \text{for } C > C_c \quad \text{(A21)} \end{cases}$$

where

S = source term

V_s = fall velocity of a sediment particle

h = flow depth

C = sediment concentration in water column

τ = bed shear stress

τ_d = critical shear stress for deposition

C_c = critical concentration = 300 mg/ℓ

30. If the bed shear stress is greater than the critical value for particle erosion τ_e, material is removed from the bed. The source term is then computed by Ariathurai's (Ariathurai, MacArthur, and Krone 1977) adaptation of Partheniades' (1962) findings:

$$S = \frac{P}{h}\left(\frac{\tau}{\tau_e} - 1\right) \quad \text{for } \tau > \tau_e \quad \text{(A22)}$$

where P is the erosion rate constant, unless the shear stress is also greater than the critical value for mass erosion. When this value is exceeded, mass failure of a sediment layer occurs and

$$S = \frac{T_L P_L}{h\Delta t} \quad \text{for } \tau > \tau_s \tag{A23}$$

where

T_L = thickness of the failed layer

P_L = density of the failed layer

Δt = time interval over which failure occurs

τ_s = bulk shear strength of the layer

31. The cohesive sediment bed consists of 1 to 10 layers, each with a distinct density and erosion resistance. The layers consolidate with overburden and time.

Bed shear stress

32. Bed shear stresses are calculated from the flow speed according to one of four optional equations: the smooth-wall log velocity profile or Manning equation for flows alone; and a smooth bed or rippled bed equation for combined currents and wind waves. Shear stresses are calculated using the shear velocity concept where

$$\tau_b = \rho u_*^2 \tag{A24}$$

where

τ_b = bed shear stress

u_* = shear velocity

and the shear velocity is calculated by one of four methods:

a. Smooth-wall log velocity profiles

$$\frac{\bar{u}}{u_*} = 5.75 \log \left(3.32 \frac{u_* h}{\nu} \right) \tag{A25}$$

which is applicable to the lower 15 percent of the boundary layer when

$$\frac{u_* h}{\nu} > 30$$

where $\bar{u}$ is the mean flow velocity (resultant of u and v components)

b. The Manning shear stress equation

$$u_* = \frac{(\bar{u}n)\sqrt{g}}{CME\ (h)^{1/6}} \tag{A26}$$

where CME is a coefficient of 1 for SI (metric) units and 1.486 for non-SI units of measurement.

c. A Jonsson-type equation for surface shear stress (plane beds) caused by waves and currents

$$u_* = \sqrt{\frac{1}{2}\left(\frac{f_w u_{om} + f_c \bar{u}}{u_{om} + \bar{u}}\right)\left(\bar{u} + u_{om}\right)^2} \tag{A27}$$

where

f_w = shear stress coefficient for waves

u_{om} = maximum orbital velocity of waves

f_c = shear stress coefficient for currents

d. A Bijker-type equation for total shear stress caused by waves and current

$$u_* = \sqrt{\frac{1}{2} f_c \bar{u}^2 + \frac{1}{4} f_w u_{om}^2} \tag{A28}$$

Solution method

33. Equation A5 is solved by the finite element method using Galerkin weighted residuals. Like RMA-2V, which uses the same general solution technique, elements are quadrilateral and may have parabolic sides. Shape functions are quadratic. Integration in space is Gaussian. Time-stepping is performed by a Crank-Nicholson approach with a weighting factor (θ) of 0.66.

A front-type solver similar to that in RMA-2V is used to solve the simultaneous equations.

REFERENCES

Ackers, P., and White, W. R. 1973. (Nov). "Sediment Transport: New Approach and Analysis," Journal, Hydraulics Division, American Society of Civil Engineers, No. HY-11.

Ariathurai, R., MacArthur, R. D., and Krone, R. C. 1977 (Oct). "Mathematical Model of Estuarial Sediment Transport," Technical Report D-77-12, US Army Engineer Waterways Experiment Station, Vicksburg, MS.

Krone, R. B. 1962. "Flume Studies of Transport of Sediment in Estuarial Shoaling Processes," Final Report, Hydraulics Engineering Research Laboratory, University of California, Berkeley, CA.

Norton, W. R., and King, I. P. 1977 (Feb). "Operating Instructions for the Computer Program RMA-2V," Resource Management Associates, Lafayette, CA.

Partheniades, E. 1962. "A Study of Erosion and Deposition of Cohesive Soils in Salt Water," Ph.D. Dissertation, University of California, Berkeley, CA.

Swart, D. H. 1976 (Sep). "Coastal Sediment Transport, Computation of Longshore Transport," R968, Part 1, Delft Hydraulics Laboratory, The Netherlands.

Thomas, W. A., and McAnally, W. H., Jr. 1985 (Aug). "User's Manual for the Generalized Computer Program System; Open-Channel Flow and Sedimentation, TABS-2, Main Text and Appendices A through O," Instruction Report HL-85-1, US Army Engineer Waterways Experiment Station, Vicksburg, MS.

White, W. R., Milli, H., and Crabbe, A. D. 1975. "Sediment Transport Theories: An Appraisal of Available Methods," Report Int 119, Vols 1 and 2, Hydraulics Research Station, Wallingford, England.

APPENDIX B: DESCRIPTION OF THE NUMERICAL MODEL, DIFID*

Model Origin

1. The instantaneous dump model (DIFID) was developed by Brandsma and Divoky (1976) for the US Army Engineer Waterways Experiment Station (WES) under the Dredged Material Research Program. Much of the basis for the model was provided by earlier model development by Koh and Chang (1973) for the barged disposal of wastes in the ocean. That work was conducted under funding by the Environmental Protection Agency in Corvallis, Oregon. Modifications to the original model have been made by the Hydraulics Laboratory at WES.

Model Approach

2. The model simulates movement of the disposed material as it falls through the water column, spreads over the bottom, and finally is transported and diffused as suspended sediment by the ambient current. DIFID is designed to simulate the movement of material from an instantaneous dump which falls as a hemispherical cloud. Thus the total time required for the material to leave the disposal vessel should not be substantially greater than the time required for the material to reach the bottom.

3. The model requires that the dredged material be broken into various solid fractions with a settling velocity specified for each fraction. In many cases, a significant portion of the material falls as "clumps" which may have a settling velocity of perhaps 1.0 to 5.0 fps. This is especially true if the dredging is done by clamshell and can be true in the case of hydraulically dredged material if consolidation takes place in the hopper during transit to the disposal site. The specification of a "clump" fraction is rather subjective; therefore the inability to accurately characterize the disposed material in some disposal operations prevents a quantitative interpretation of model results in those operations.

4. As noted, a settling velocity must be prescribed for each solid fraction. A basic assumption is that unless the fraction is specified as being cohesive, in which case the settling velocity is computed as a function of

---

* Taken from Trawle and Johnson (1986), pp 7-18.

concentration, the settling is considered to occur at a constant rate. In other words, hindered settling is not taken into consideration.

5. Although a variable water depth is allowed over the long-term grid, the collapse of the dredged material cloud on the bottom is somewhat restricted. The effect of a bottom slope is allowed through the incorporation of a gravitational force in the computation of the collapsing cloud. However, a basic limitation still exists in that the bottom is assumed to slope in only one direction over the collapsed region; e.g., bottom collapse on a "mound" where the collapsing cloud runs down the sides is not treated.

6. A major limitation of the model is the basic assumption that once solid particles are deposited on the bottom they remain there. Therefore the model should only be applied over time frames in which erosion of the newly deposited material is insignificant.

7. The model allows for two separate treatments of the passive transport and diffusion phase. In one method, material from the convective descent and dynamic collapse phases is inserted into the fixed long-term grid. Therefore computations at each point of the grid must be made at each time-step in order to march the solution from one time-step to the next. Solid bodies in the field and boundary effects are treated. However, disadvantages are that the vertical distribution is assumed to be that of a "top hat" profile, grid dispersion errors may occur, and the computations can become costly for large grids if many time-steps are computed. A "top hat" profile is represented by a step function that does not allow for any gradual change over the water column. The second approach is to allow material from the descent and collapse phases to be stored in small Gaussian clouds. These clouds are then diffused and transported at the end of each time-step. Computations on the long-term grid are only made at those times when output is desired. However, a limitation when using this approach is that horizontal solid boundaries are not allowed in the long-term grid. This limitation could be removed by employing reflection principles as is currently done at the surface and the bottom.

Theoretical Basis

8. The behavior of the disposed material is assumed to be separated into three phases: convective descent, during which the dump cloud or discharge jet falls under the influence of gravity; dynamic collapse, occurring

when the descending cloud either impacts the bottom or arrives at the level of neutral buoyancy at which descent is retarded and horizontal spreading dominates; and long-term passive dispersion, commencing when the material transport and spreading are determined more by ambient currents and turbulence than by the dynamics of the disposal operation. Figure B1 illustrates these phases.

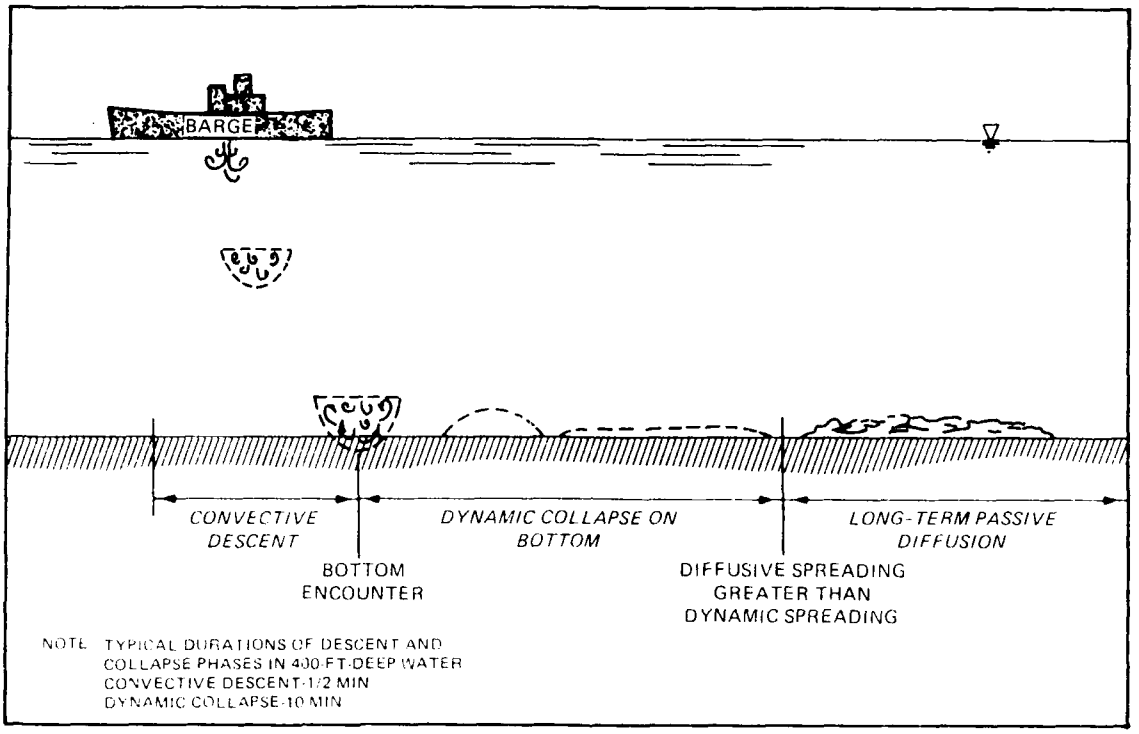

Figure B1. Illustration of idealized bottom encounter after instantaneous dump of dredged material (from Brandsma and Divoky 1976)

Convective descent

9. A single cloud that maintains a hemispherical shape during convective descent is assumed to be released. Since the solids concentration in discharged dredged material is usually low, the cloud is expected to behave as a dense liquid; thus a basic assumption is that a buoyant thermal analysis is appropriate. The equations governing the motion are those for conservation of mass, momentum, buoyancy, each solid, and vorticity. The equations are straightforward statements of conservation principles and are presented by Brandsma and Divoky (1976). It should be noted that the entrainment coefficient associated with the entrainment of ambient fluid into the descending hemispherical cloud is assumed to vary smoothly between its value for a vortex

ring and the value for turbulent thermals. Model results are quite sensitive to the entrainment coefficient, which in turn is dependent upon the material being dumped (the higher the moisture content, the larger the value of the entrainment coefficient).

Dynamic collapse

10. During convective descent, the dumped material cloud grows as a result of entrainment. Eventually, either the material reaches the bottom or the density difference between the discharged material and the ambient fluid becomes small enough for a position of neutral buoyancy to be assumed. In either case, the vertical motion is arrested and a dynamic spreading in the horizontal direction occurs. The basic shape assumed for the collapsing cloud is an oblate spheroid. With the exception of vorticity, which is assumed to have been dissipated by the stratified ambient water column, the same conservation equations used in convective descent but now written for an oblate spheroid are applicable. For the case of collapse on the bottom, the cloud takes the shape of the general ellipsoid and a frictional force between the bottom and collapsing cloud is included.

Long-term transport diffusion

11. The long-term dispersion phase is treated in one of two ways. When the rate of horizontal spreading in the dynamic collapse phase becomes less than an estimated rate of spreading due to turbulent diffusion, the collapse phase is terminated. During collapse, solid particles can settle as a result of their fall velocity. As these particles leave the main body of material, they are stored in small clouds that are characterized by a uniform concentration, thickness, and position in the water column. In the first method of handling the transport-diffusion computations, these small clouds are allowed to settle and disperse until they become large enough to be inserted into the grid positioned in the horizontal plane. Once small clouds are inserted at particular grid points, these points then have a concentration, thickness, and top position associated with them. Figure B2 illustrates a typical concentration profile at a grid point. Computations on the grid are made using a backward convection scheme rather than attempting a numerical solution of the governing convection-diffusion equation. In the backward convection solution technique, a massless particle at each grid point at the present level is moved backward in time by the ambient current to the position it occupied one time-step before. The concentration at the grid point it presently occupies

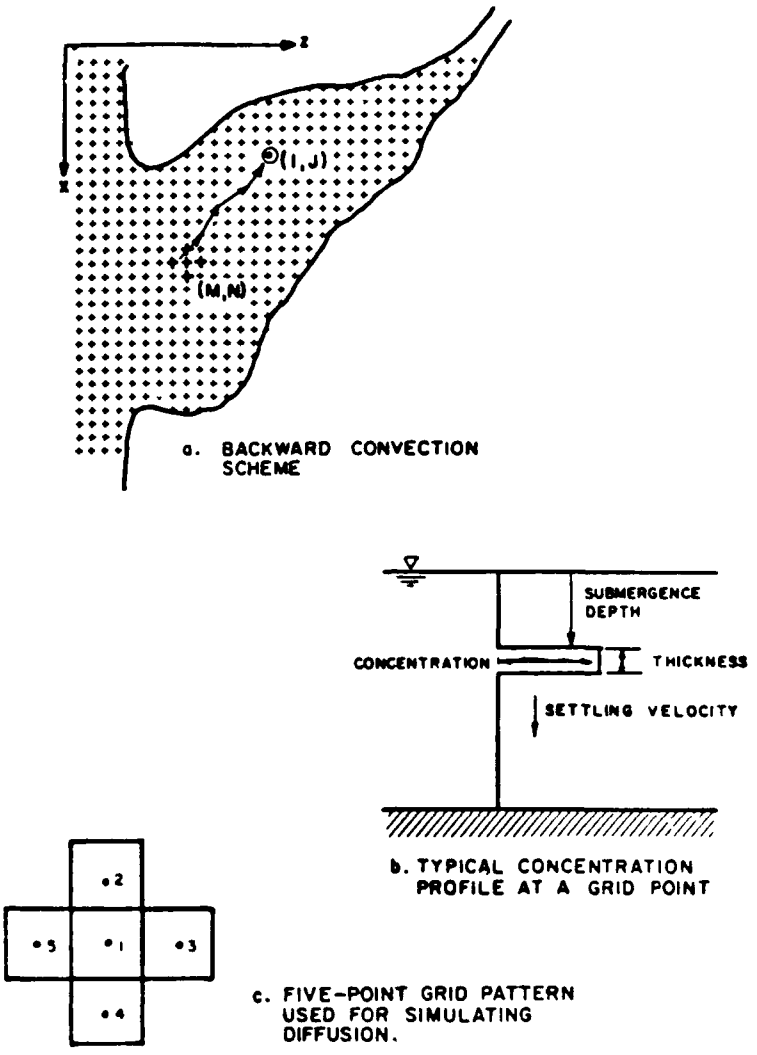

Figure B2. Aspects of passive diffusion
(from Brandsma and Divoky 1976)

is then taken as a five-point average of points surrounding its old position.

12. Rather than making computations at each point of the long-term grid at each time-step, an alternative method for handling the transport-diffusion computations has been incorporated that only uses the horizontal grid for output purposes. The idea for this method was obtained from work by Brandsma and Sauer (1983), on the development of a drilling mud model. Rather than inserting the mass from the previously discussed small clouds into the horizontal grid, each small cloud is assumed to have a Gaussian distribution given by

$$C_c = \frac{m}{(2\pi)^{3/2}\sigma_x\sigma_y\sigma_z} \exp\left[-\frac{1}{2}\left(\frac{(x-x_o)^2}{\sigma_x^2} + \frac{(y-y_o)^2}{\sigma_y^2} + \frac{(z-z_o)^2}{\sigma_z^2}\right)\right] \quad (B1)$$

where

x,y,z = spatial coordinates

x_o,y_o,z_o = coordinates of cloud centroid

$\sigma_x,\sigma_y,\sigma_z$ = standard deviations

m = total mass of cloud in ft^3

At the end of each time-step, each cloud is advected horizontally by the input velocity field. The new position of the cloud centroid is determined by

$$x_{o_{new}} = x_{o_{old}} + u \cdot \Delta t$$

$$z_{o_{new}} = z_{o_{old}} + w \cdot \Delta t \quad (B2)$$

where

u,w = local ambient velocities in ft/sec

Δt = long-term time-step in sec

13. In addition to the advection or transport of the cloud, the cloud grows both horizontally and vertically as a result of turbulent diffusion. The horizontal diffusion is based upon the commonly assumed 4/3 power law. Therefore, the diffusion coefficient is given as

$$K_{x,z} = A_L L^{4/3} \quad (B3)$$

where A_L is an input dissipation parameter and L is set equal to four standard deviations. The expression for the horizontal growth of a cloud then becomes

$$\sigma_{x,z_{new}} = \sigma_{x,z_{old}} \left(1 + 4^{4/3}\,\frac{2}{3}\,\frac{A_L \Delta t}{\sigma_{x,z_{old}}^{2/3}}\right)^{3/2} \quad (B4)$$

14. Vertical growth is similarly achieved by employing the Fickian expression

$$\sigma_y = (2K_y t)^{1/2} \tag{B5}$$

where

K_y = vertical diffusion coefficient

t = time since formation of the cloud

From Equation B5,

$$\frac{d\sigma_y}{dt} = K_y (2K_y t)^{-1/2} = \frac{K_y}{\sigma_y} \tag{B6}$$

and thus,

$$\sigma_{y_{new}} = \sigma_{y_{old}} + \frac{K_y}{\sigma_{y_{old}}} \Delta t \tag{B7}$$

where K_y is a function of the stratification of the water column. The maximum value of K_y is input as a model coefficient and occurs when the water density is uniform.

15. If long-term output is desired at the end of a particular time-step, the concentration of each solid type is given at each grid point by summing the contributions from individual clouds as

$$C_t = (2\pi)^{-3/2} \sum_{i=1}^{N} \left\{ \frac{m_i}{\sigma_{x_i} \sigma_{y_i} \sigma_{z_i}} \times \exp\left[-\frac{1}{2} \left(\frac{(x - x_{o_i})^2}{\sigma_{x_i}^2} + \frac{(y - y_{o_i})^2}{\sigma_{y_i}^2} + \frac{(z - z_{o_i})^2}{\sigma_{z_i}^2} \right) \right] \right\} \tag{B8}$$

where N is the number of small clouds of a particular solid type and y (the vertical position at which output is desired) is specified through input data.

16. At the present time, the effect of horizontal solid boundaries has not been included. Therefore the Gaussian cloud method of transport-diffusion computations should only be used if solid boundaries are far removed from the suspended material. However, such an effect due to the bottom and the water surface has been included in the vertical. This is accomplished through reflection principles by assuming that identical clouds lie above the water surface and below the bottom.

17. In addition to the horizontal advection and diffusion of material, settling of the suspended solids also occurs. Therefore, at each net point the amount of solid material deposited on the bottom and a corresponding thickness are also determined. A basic assumption in the models is that once material is deposited on the bottom it remains there, i.e., neither erosion nor stable-bed movement of material is allowed. This is the primary theoretical limitation of the models that restricts their usefulness to the study of the short-term fate of discharged material.

Model Capabilities

18. The computer programs enable the computation of the physical fate of dredged material disposed in open water. The following discussion describes particular capabilities or special features of the codes.

Ambient environment

19. A wide range of ambient conditions are allowed in model computations. Conditions (ranging from those found in relatively shallow and well-mixed bays and estuaries to highly stratified two-layer flow fields, found in estuaries where salt wedges are formed) can be variable from one long-term grid cell to the next. The only restriction on bottom topography is that associated with the collapse phase which was discussed in paragraph B5. Any of three options of ambient current illustrated in Figure B3 may be selected, with the simplest case being the time-invariant profiles shown in Figure B3a for a constant depth disposal site. The ambient density profile is input as a function of water depth at the deepest point in the disposal site. This profile may vary with time but is the same at each point of the grid.

Time-varying fall velocities

20. If a solid fraction is specified as being cohesive, the settling velocity is computed as a function of the suspended sediment concentration of

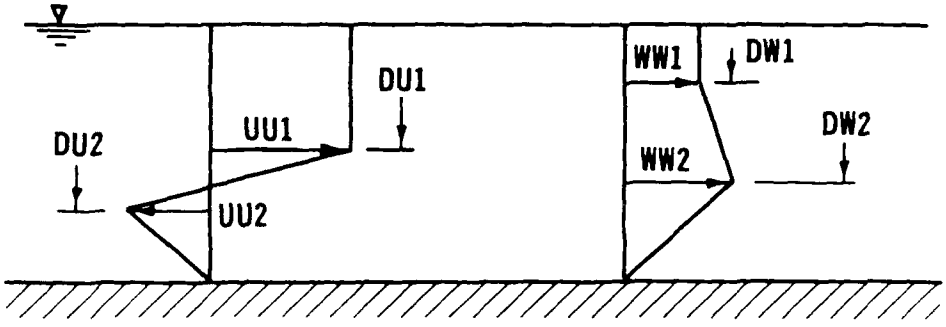

a. SIMPLE ORTHOGONAL VELOCITY PROFILES FOR CONSTANT DEPTH. APPLIED EVERYWHERE IN FIELD

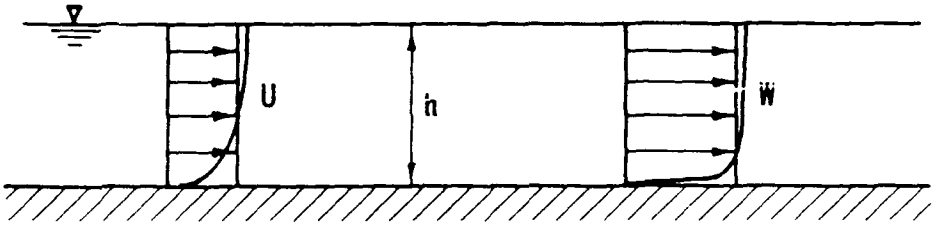

b. VERTICALLY AVERAGED VELOCITY PROFILES FOR VARIABLE DEPTHS WITH EQUIVALENT LOGARITHMIC PROFILES SUPERIMPOSED.

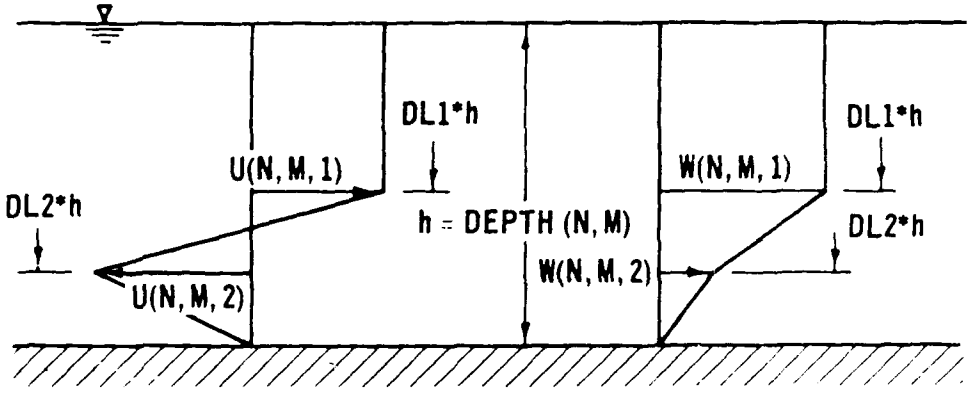

c. TWO-LAYER PROFILES FOR VARIABLE DEPTH

Figure B3. Illustration of the various velocity profiles available for use in models (from Brandsma and Divoky 1976)

that solid type. The following algorithm is currently used

$$V_s \begin{cases} = 0.0017 \quad \text{if} \quad C \leq 25 \text{ mg/}\ell \\ = 0.00713\ C^{4/3}/304.8 \quad \text{if} \quad 25 \leq C \leq 300 \text{ mg/}\ell \\ = 0.047 \quad \text{if} \quad C > 300 \text{ mg/}\ell \end{cases} \tag{B9}$$

where

V_s = settling velocity, ft/sec

C = suspended sediment concentration, mg/ℓ

Conservative constituent computations

21. The models allow for the dredged material to contain a conservative constituent with a nonzero background concentration of that constituent. Computing the resultant time-history of that concentration provides information on the dilution that can be expected over a period of time at the disposal site.

Output available

22. Through input data the user specifies the amount of output desired. Much of the input data required, e.g., the water depth field, are immediately printed after being read. At the end of the convective descent phase, the location of the cloud centroid, the velocity of the cloud centroid, the radius of the hemispherical cloud, the density difference between the cloud and the ambient water, the conservative constituent concentration, and the total volume and concentration of each solid fraction are provided as functions of time since release of the material.

23. At the conclusion of the collapse phase, time-dependent information concerning the size of the collapsing cloud, its density, and its centroid location and velocity as well as conservative constituent and solids concentrations can be requested.

24. At various times, as requested through input data, output concerning suspended sediment concentrations and solids deposited on the bottom can be obtained from the transport-diffusion computations. If the backward convection long-term scheme is employed, the suspended sediment concentration and the location of its "top hat" profile (Figure B2b) are provided at each grid point for each sediment fraction. However, if the Gaussian cloud long-term scheme is selected, only concentrations at the water depths requested are

provided at each long-term grid point. In both cases, the volume of each sediment fraction that has been deposited in each grid cell is provided. At the conclusion of the simulation, a voids ratio specified through input data is used to compute the thickness of the deposited material.

Assembly of Input Data

25. Depending upon the complexity of ambient conditions at the disposal site, the preparation of input data can range from requiring the application of a three-dimensional model to provide stratified velocity fields to a simple input data setup of perhaps 20 to 25 lines. Input data can be grouped into (a) a description of the ambient environment at the disposal site, (b) characterization of the dredged material, (c) data describing the disposal operation, and (d) model coefficients.

Disposal site data

26. The first task to be accomplished when applying the model is that of constructing a horizontal grid over the disposal site. The number of grid points should be kept as small as possible but large enough to extend the grid beyond the area of interest at the level of spatial detail desired. Quite often one may wish to change the horizontal grid after a few preliminary runs. Water depths and the horizontal components of the ambient current must be at each grid point. Any of the three options of velocity input illustrated in Figure B3 may be selected, with the simplest case being velocities at a constant depth disposal site. The ambient density profile at the deepest point in the disposal site must also be input. This profile may vary with time but is assumed to be the same at each point of the grid.

Characterization of dredged material

27. The dredged material can be composed of up to 12 solid fractions, a fluid component, and a conservative chemical constituent. For each solid fraction, its concentration by volume, density, fall velocity, voids ratio, and an indicator as to whether or not the fraction is cohesive must be input. Proper material characterization is extremely important in obtaining realistic predictions from the models. If a conservative chemical constituent is to be traced, its initial concentration and a background concentration must be given. In addition, the bulk density and aggregate voids ratio of the dredged material must be prescribed along with its liquid limit.

Disposal operations data

28. Information required includes the position of the barge or scow on the horizontal grid, the volume of material dumped, and the loaded and unloaded draft of the disposal vessel.

Model coefficients

29. There are 14 coefficients in DIFID. Default values are contained in the computer code that reflect the model developer's best guess. However, the user may input other values. Computer experimentation such as that presented by Johnson and Holliday (1978) has shown that results appear to be fairly insensitive to many of the coefficients. The most important coefficients are drag coefficients in the convective descent and collapse phases as well as coefficients governing the entrainment of ambient water into the dredged material cloud.

REFERENCES

Brandsma, M. G., and Divoky, D. J. 1976 (May). "Development of Models for Prediction of Short-Term Fate of Dredged Material Discharged in the Estuarine Environment," Contract Report D-76-5, US Army Engineer Waterways Experiment Station, Vicksburg, MS.

Brandsma, M. G., and Sauer, T. C., Jr. (1983). "Mud Discharge Model - Report and User's Guide," Exxon Production Research Company, Houston, TX.

Johnson, B. H., and Holliday, B. W. 1978. "Evaluation and Calibration of Tetra Tech Dredged Material Disposal Models Based on Field Data," Technical Report D-78-47, US Army Engineer Waterways Experiment Station, Vicksburg, MS.

Koh, R. C. Y., and Chang, Y. C. 1973 (Dec). "Mathematical Model for Barged Ocean Disposal of Waste," Environmental Protection Technology Series EPA 660/2-73-029, US Environmental Protection Agency, Washington, DC.

Trawle, M. J., and Johnson, B. H. 1986 (Mar). "Alcatraz Disposal Site Investigation," Miscellaneous Paper HL-86-1, US Army Engineer Waterways Experiment Station, Vicksburg, MS.